A mechanistic model of microbially mediated soil biogeochemical processes - a reality check

Simone Fatichi[1], Stefano Manzoni[2,3], Dani Or[4], and Athanasios Paschalis[5]

[1]Institute of Environmental Engineering, ETH Zurich, Switzerland
[2]Department of Physical Geography, Stockholm University, Sweden
[3]Bolin Centre for Climate Research, Stockholm, Sweden
[4]Department of Environmental Science, Institute of Biogeochemistry and Pollutant Dynamics , ETH Zurich, Switzerland
[5]Department of Civil and Environmental Engineering, Imperial College London, UK

Key Points:

- We introduce a new microbial-explicit soil biogeochemistry module into a terrestrial biosphere model
- Uncalibrated model simulations compared favorably with global patterns of soil biogeochemistry processes
- Results offer mechanistic estimates of microbe contribution to soil respiration and carbon dynamics

Corresponding author: Simone Fatichi, simone.fatichi@ifu.baug.ethz.ch

Abstract

Present gaps in the representation of key soil biogeochemical processes such as the partitioning of soil organic carbon (SOC) among functional components, microbial biomass and diversity, and the coupling of carbon and nutrient cycles present a challenge to improving the reliability of projected soil carbon dynamics. We introduce a new soil biogeochemistry module linked with a well-tested terrestrial biosphere model T&C. The module explicitly distinguishes functional SOC components. Extracellular enzymes and microbial pools are differentiated based on the functional roles of bacteria, saprotrophic, and mycorrhizal fungi. Soil macrofauna is also represented. The model resolves the cycles of nitrogen, phosphorus, and potassium. Model simulations for 20 sites compared favorably with global patterns of litter and soil stoichiometry, microbial and macrofaunal biomass relations with soil organic carbon, soil respiration and nutrient mineralization rates. Long-term responses to bare fallow and nitrogen addition experiments were also in agreement with observations. Some discrepancies between predictions and observations are appreciable in the response to litter manipulation. Upon successful model reproduction of observed general trends, we assessed patterns associated with the carbon cycle that were challenging to address empirically. Despite large site-to-site variability, fine root, fungal, bacteria, and macrofaunal respiration account for 33%, 40%, 24% and 3% on average of total belowground respiration, respectively. Simulated root exudation and carbon export to mycorrhizal fungi represent on average about 13% of plant net primary productivity (NPP). These results offer mechanistic and general estimates of microbial biomass and its contribution to respiration fluxes and to soil organic matter dynamics.

1 Introduction

The potential of an ecosystem to store and release carbon is inherently linked to soil biogeochemical processes among other factors (Raich & Nadelhoffer, 1989; Raich & Schlesinger, 1992; Schimel, 2013; Schmidt et al., 2011; Trumbore & Czimczik, 2008). Quantification of environmental controls on soil carbon turnover rates and a more accurate representation of soil biogeochemistry have been recognized as a key challenge to reducing uncertainties in land-carbon climatic feedbacks and improving future projections of climate change (e.g., Friedlingstein et al., 2014; Thornton, Lamarque, Rosenbloom, & Mahowald, 2007; Todd-Brown et al., 2014, 2013; Zaehle & Dalmonech, 2011). Consequently, contemporary studies have followed two general approaches. The first is data-driven where spatial and temporal patterns of soil carbon are empirically inferred (Carvalhais et al., 2014; Hashimoto et al., 2015), such as the recent study of Crowther et al. (2016) for quantifying global soil carbon losses to warming by extrapolating observed sensitivities in field manipulation experiments. The alternative approach, adopted in this study, invokes mechanistic models of soil biogeochemistry to enhance process understanding or make predictions (e.g., Abramoff et al., 2018; Goll et al., 2012; Manzoni, Moyano, Kätterer, & Schimel, 2016; Robertson et al., 2019; Tang, Riley, Koven, & Subin, 2013; Y.-P. Wang, Houlton, & Field, 2007; Zhu, Riley, Tang, & Koven, 2016). Traditionally models have represented soil organic carbon by assigning it to three pools: fast, slow, and passive (Foley, 1995; Krinner et al., 2005; Parton, Stewart, & Cole, 1988; Sato, Itoh, & Kohyama, 2007; Sitch et al., 2003). These pools are often characterized by linear kinetics and different decay rates in an attempt to preserve variability in decomposition for various degrees of soil organic protection or recalcitrance of the substrate (Freschet, Aerts, & Cornelissen, 2012; Talbot & Treseder, 2012). Therefore, first generation models often did not distinguish between substrate and microbial biomass and implicitly assumed that microbial biomass is not a limiting factor in the rates of SOC decomposition. Simplifying soil organic carbon representation by lumping together different functional components in a few pools creates a discrepancy between modeled quantities and measurable SOC fractions in the soil and it does not allow to properly represent physical and biochemical processes (Schmidt et al., 2011; Six et al., 2001).

Following the work of Schimel and Weintraub (2003), recent model developments have been devoted to explicitly represent the role of microbial biomass and extracellular enzymes in soil carbon dynamics (Abramoff et al., 2018; Allison, Wallenstein, & Bradford, 2010; Manzoni & Porporato, 2009; Orwin, Kirschbaum, St John, & Dickie, 2011; Wieder, Allison, et al., 2015; Wieder, Bonan, & Allison, 2013; Wieder, Grandy, Kallenbach, & Bonan, 2014; Wieder, Grandy, Kallenbach, Taylor, & Bonan, 2015). Other efforts aimed at including more mechanistic representation of nutrient cycles such as nitrogen (Koven et al., 2013; Xu-Ri & Prentice, 2008; Yang, Wittig, Jain, & Post, 2009; Zaehle & Friend, 2010) and phosphorus (Buendia, Kleidon, & Porporato, 2010; Goll et al., 2017; Runyan & D'Odorico, 2012; Yang, Thornton, Ricciuto, & Post, 2014), as well as plant-mycorrhizae interactions (Baskaran et al., 2017; Brzostek, Fisher, & Phillips, 2014; Shi, Fisher, Brzostek, & Phillips, 2016). Adopting a more mechanistic and better constrained description of soil biogeochemical processes has been shown to improve simulations of global-scale soil-carbon patterns (Wieder et al., 2013; Wieder, Grandy, et al., 2015). However, most model applications have remained at the level of detailed sensitivity analyses with little comparison between observations and results either from soil biogeochemistry focused models (Li, Wang, Allison, Mayes, & Luo, 2014; G. Wang, Post, & Mayes, 2013) or global scale Earth System Models. Most importantly, soil biochemical processes are deeply connected to water, energy, and vegetation dynamics above and belowground and cannot be analyzed in isolation from a land-surface model, even though projections about the fate of soil organic carbon have been often discussed without a coupling with a vegetation model (e.g., Abramoff et al., 2018; Allison et al., 2010; Frey, Lee, Melillo, & Six, 2013; Orwin et al., 2011; Tang & Riley, 2015). Probably for this reason, only few contributions challenged biogeochemistry models to reproduce the observed response to environmental manipulations (P. Smith et al., 1997; Zaehle et al., 2014). Among the potential treatments, warming (Crowther et al., 2016), bare-fallow (Barré et al., 2010; Wadman & de Haan, 1997), litter-manipulation (Bowden, Nadelhoffer, Boone, Meillo, & Garrison., 1993; Rousk & Frey, 2015), nitrogen addition (Compton, Watrud, Porteous, & DeGrood, 2004; Magill et al., 2004) and burning treatments (Ojima, Schimel, Parton, & Owensby, 1994; Wan, Hui, & Luo, 2001) have been carried out in the past and they can be used for model confirmation. Arguably, these are the most important tests to evaluate the correctness of the mechanistic structure of a model and its capability to reproduce responses to environmental changes. A model should be able to reproduce the observed dynamics under control and manipulated conditions using an identical parametrization (e.g., without specific tuning) to be considered robust in the simulation of unobserved conditions, as it is the case for projections in a future climate. Moreover, detailed data to parameterize and validate different model components are scarce, although few recent reviews of parameter values can potentially reduce this problem (Allison, 2017; G. Wang et al., 2013). How to assign different parameters for various ecosystems or soil microbial communities remains, however, particularly challenging (Bradford & Fierer, 2012), as discussed later in this article.

In this study, we introduce a new soil biogeochemistry module that has been integrated with an existing model of land-surface hydrology and vegetation dynamics, T&C (e.g., Fatichi, Ivanov, & Caporali, 2012; Fatichi & Pappas, 2017; Manoli, Ivanov, & Fatichi, 2018). Specifically, the soil biogeochemistry module is vertically lumped, it explicitly separates different litter pools and distinguishes SOC in particulate, dissolved, and mineral associated fractions, similarly to the MEND model (G. Wang et al., 2013). Extracellular enzymes and microbial pools are explicitly represented differentiating the functional roles of bacteria, saprotrophic fungi, and arbuscular and ecto- mycorrhizae. Microbial activity depends on soil temperature, soil water potential and SOC stoichiometry. The activity of macrofauna is also modeled. Nutrient dynamics include the cycles of nitrogen, phosphorus, and potassium. Nitrogen and phosphorus are essential nutrients for plant functioning and productivity (Le Bauer & Treseder, 2008; Vitousek, Porder, Houlton, & Chadwick, 2010); more recently also potassium has been shown to limit plant productivity of terrestrial ecosystems to a similar extent of nitrogen and phosphorus (Sardans

& Penuelas, 2015). The model also accounts for feedbacks between nutrient limitations and plant growth and for plant stoichiometric flexibility. In turn, litter input is a function of the simulated vegetation dynamics and thus is not prescribed. Root exudation and export to mycorrhizae are computed based on the cost of nutrient uptake similarly to the rationale of the FUN2.0 model (Brzostek et al., 2014).

In addition to the introduction of the new model and its components, this study has two additional goals. First, it aims at testing the model for a number of real case studies, highlighting strengths and limitations of this approach in the framework of Earth system models. Model parameters describing interactions among microbial and soil organic carbon pools and reactions rates are likely scale, ecosystem, and case study specific, because of the huge biodiversity in soil microbial communities (e.g., Fierer & Jackson, 2006; Nannipieri et al., 2017) and potential differences of carbon protection mechanisms in the soil (Six, Conant, Paul, & Paustian, 2002). However, we intentionally use a single parameter set for all simulations to test the suitability of such an approach for large-scale (potentially global) applications, where one or a limited set of parameter values must be forcefully used, because local tuning is impractical. While recognizing that many parameters are highly uncertain, a formal sensitivity analysis is beyond the scope here. The implications for uncertainty of using a single parameter set are, however, discussed. The new modeling tool, T&C-BG, is intended to reproduce main-differences across various ecosystems and climates as well as major responses to environmental perturbations. The model is tested against: (i) global patterns of biomass in belowground communities and functions, (ii) short-to mid-term response in soil respiration as inferred from flux-tower data; (iii) soil organic carbon responses to bare fallow and litter manipulation experiments, and (iv) ecosystem response to nitrogen addition.

The second objective is to use the modeling framework for answering a specific science question: how belowground soil respiration is partitioned among different components of belowground living biomass? The model offers new insights into the relative magnitudes of often poorly constrained quantities such as partitioning of soil respiration components among fungi, bacteria, roots, and macrofauna, and estimates of root exudation and carbon export to mycorrhizae.

2 Materials and Methods

2.1 Model description

Numerical simulations were carried using the ecosystem model T&C (Fatichi et al., 2012, 2015; Fatichi & Pappas, 2017; Fatichi, Zeeman, Fuhrer, & Burlando, 2014; Manoli et al., 2018; Mastrotheodoros et al., 2017; Pappas, Fatichi, & Burlando, 2016; Paschalis, Fatichi, Katul, & Ivanov, 2015; Paschalis, Fatichi, Pappas, & Or, 2018) combined with new modules simulating soil biogeochemistry and plant nutrient dynamics (T&C-BG) described in the following and extensively in the Supp. Information: Fig. S1, Text S1 and S2, and additional references in the Supp. Information (Ainsworth & Long, 2005; Batterman et al., 2013; Chapin III, Schulze, & Mooney, 1990; Curry & Schmidt, 2007; Daly & Porporato, 2005; Farquhar, Caemmerer, & Berry, 1980; Friend, Stevens, Knox, & Cannell, 1997; Hanson, Allison, Bradford, Wallenstein, & Treseder, 2008; Hassink & Whitmore, 1997; Jackson, Mooney, & Schulze, 1997; Jungk, 2002; Kögel-Knabner, 2002; Manzoni, 2017; Manzoni, Jackson, Trofymow, & Porporato, 2008; Manzoni & Porporato, 2009; Manzoni, Schimel, & Porporato, 2012; Manzoni, Vico, Katul, Palmroth, & Porporato, 2014; Moorhead & Sinsabaugh, 2006; Moyano, Manzoni, & Chenu, 2013; Phillips, Brzostek, & Midgley, 2013; Poorter, 1994; Poorter & Villar, 1997; Roumet et al., 2016; Sinsabaugh, Manzoni, Moorhead, & Richter, 2013; S. E. Smith & Read, 2008; S. E. Smith & Smith, 2011; Sparks & Carski, 1985; Stewart, Paustian, Conant, Plante, & Six, 2007; H. Thomas & Stoddart, 1980; S. C. Thomas & Martin, 2012; Yang, Post, Thornton, & Jain, 2013; Zhang et al., 2018). The original T&C is a mechanistic model simulating en-

ergy, water, and CO_2 exchanges at the land surface at an hourly time step. Even though the model can be used for distributed simulations over a catchment, here it is applied at the plot-scale, e.g., as one-dimensional vertical model. Mass and energy fluxes control the temporal dynamics of vegetation (carbon pools) that in turn affect land-atmosphere exchange through its biophysical structure and physiological properties. For instance, the Leaf Area Index (LAI) is a prognostic variable, which varies in response to environmental conditions and vegetation phenology, which is also simulated. Changes in LAI can affect water and carbon fluxes that in turn modify vegetation growth in a fully interactive framework. The soil column is discretized in a number of vertical layers, with increasing depth from near the surface to the bedrock. Heterogeneity in the soil hydraulic and thermal properties in the vertical direction can be accounted for. Fine root biomass is distributed vertically with an exponential profile up to a maximum rooting depth.

2.1.1 Plant nutrient dynamics

Changes in plant total nutrient content depend on changes in the carbon pools (e.g., leaves, living sapwood, fine roots, carbohydrate reserves, flower and fruits, and heartwood) and of the stoichiometry of the various pools. Each carbon pool has a corresponding quantity of nutrients necessary for its construction, but nutrients can be also stored in the plant as reserves. In fact, stoichiometric ratios of different tissues are flexible and respond to nutrient availability (Magill et al., 2004; Sistla & Schimel, 2012; Zaehle et al., 2014). The target stoichiometric ratios are prescribed in the model and define the quantity of nutrients required for a given amount of carbon in a plant with a balanced nutrient status. Stoichiometric flexibility is explicitly modeled as a two-step processes. First, nutrient reserves can buffer uptake and demand of N, P, and K without modifying the corresponding concentration of structural (wood) and non-structural (leaves, fine roots, fruit and flowers pools) tissues. Second, tissue concentration in the non-structural compartments can be modified to respond to excess or deficit of nutrients, allowing for a real stoichiometric flexibility (see Supp. Information). Note that this implies that in the first phase nutrient reserves are changing somewhere within the plant without affecting the nutrient concentration of non-structural pools. If nutrient reserves exceed the maximum nutrient reserve size, nutrient concentrations in non-structural compartments increase, while if the modeled nutrient reserves decrease, the nutrient concentrations in the non-structural compartments falls below the target value (see Supp. Information for a detailed description). The nutrient budget of the plant is thus obtained computing changes in nutrient reserves of nitrogen (N), phosphorus (P), and potassium (K). In certain cases, insufficient nutrient availability may prevent building plant tissues, leading to nutrient constraints on plant growth. Under normal conditions, such a modeling solution allows to maintain a relatively stable nutrient concentration through time in the various plant compartments, as it is often observed in reality. Furthermore, even under unusual conditions (e.g., a nutrient manipulation experiment) the model maintains the relative nutrient concentration with respect to the target value constrained mostly between -35% to +60%, consistent with observed stoichiometric flexibility of non-structural tissues (Meyerholt & Zaehle, 2015). The model also accounts for the fact that changes in leaf nitrogen concentration affects leaf photosynthetic capacity (Bonan et al., 2011; Clark et al., 2011; Friend & Kiang, 2005; Oleson et al., 2013; Zaehle & Friend, 2010) and that maintenance respiration in various pools is related to their nitrogen concentrations (Ruimy, Dedieu, & Saugier, 1996; Ryan, 1991). However, in T&C-BG these controls are dampened in comparison to what assumed by other models (see Supp. Information).

The nutrient amount exported from plant tissues is related to the turnover rates of carbon pools and to the tissue stoichiometry. Nutrient resorption from leaves and fine roots (Cleveland et al., 2013; Reed, Townsend, Davidson, & Cleveland, 2012; Vergutz, Manzoni, Porporato, Novais, & Jackson, 2012) is modeled as constant fractions of the pool nutrient content, except when there is a nutrient surplus (see Supp. Information). Uptake of mineral nutrients can occur directly from fine roots and it can be passive, i.e.,

following the transpiration flow, or active. i.e., against concentration gradients (e.g., Haynes, 1990; Porporato, D'Odorico, Laio, & Rodriguez-Iturbe, 2003). Additionally, mycorrhizal symbiosis contributes significantly to the uptake of nutrients (Hinsinger et al., 2011; Marschner & Dell, 1994). The actual nutrient uptake rates are computed as the maximum between passive uptake occurring through the transpiration stream and active uptake influenced by the amount and biophysical properties of fine root and ectomycorrhizal and arbuscular mycorrhizal fungi (Supp. Information). Suppression functions for nutrient uptake are introduced to gradually decrease plant uptake when its nutrient concentration is above a given threshold.

Computation of root exudation, carbon export to mycorrhiza and carbon allocated to the root-nodules for biological nitrogen fixation (BFN) follows the rationale of the FUN2.0 model presented by Fisher et al. (2010) and Brzostek et al. (2014). The original FUN2.0 model delineates a resistor network for the cost of nitrogen acquisition, corresponding to the amount of nitrogen needed to support net primary production and computes the integrated carbon costs across a series of pathways, where the amount of carbon spent in each pathway depends on the resistance through that pathway (Brzostek et al., 2014). The FUN2.0 scheme is modified for T&C-BG since foliar nutrient re-translocation and nutrient uptake rates are accounted for in a different way, and not only nitrogen uptake but also phosphorus and potassium uptake rates are considered. Furthermore, T&C-BG has to compute carbon exports at the daily scale, while FUN2.0 operates at the annual scale. Specifically, beyond root respiration, T&C-BG includes costs related to non-mycorrhizal active nutrient uptake, represented by root exudation, which depend on soil nutrient content and fine root biomass; the costs for ectomycorrhizal, and arbuscular mycorrhizal active nutrient uptake correspond to the carbon cost of growth and maintenance of mycorrhizae and depend on soil nutrient availability and mycorrhizal biomass. Finally, the cost of biological nitrogen fixation depends on soil temperature as in the original FUN2.0 model. A full description of the root exudation and carbon export to mycorrhiza is presented in the Supp. Information.

2.1.2 Litter budget

Litter is produced as a consequence of plant tissue turnover (e.g., leaf fall, self-pruning) due to ageing and environmental stresses or because of disturbances and management actions and it is computed as an integral component of the original T&C model. The total plant N, P, K export is therefore a function of tissue turnover rates, stoichiometry, and resorption coefficients, i.e., the nutrient translocated from senescing leaves to other plant tissues (see Supp. Information). The total carbon exported by the plant in litter form is subdivided in eight fluxes, which serve as inputs to the litter pools in addition to the carbon exported to mycorrhizal associations. Eight distinct carbon fluxes are necessary because litter is subdivided between belowground and aboveground compartments and among woody, metabolic, and structural components. The structural and woody litter is in turn chemically subdivided into non-lignin and lignin components. The woody litter is separated from structural litter only in the aboveground, while in the belowground compartment woody debris are assumed to contribute directly to metabolic and structural litter. This subdivision largely follows a modified version of the CENTURY model (Kirschbaum & Paul, 2002). The fraction of metabolic versus structural litter is computed for each pool based on the lignin to nitrogen ratio (Krinner et al., 2005; Orwin et al., 2011; Parton et al., 1988). Progressively more carbon is allocated to structural litter when the lignin concentration of the tissue increases or the nitrogen concentration decreases. Nutrients are only allocated to three litter pools (aboveground, belowground and aboveground woody).

The organic carbon decomposition rates of the eight litter pools are assumed to follow linear kinetics as in the original version of the CENTURY model and subsequent modifications (Kirschbaum & Paul, 2002; Parton et al., 1993, 1988). This assumption relies

on the fact that microbial communities are typically not representing a limiting factor for aboveground (air-exposed) litter decomposition, and therefore decomposition rates can be assumed to scale linearly with the litter mass. Interactions with macrofauna are also neglected, even though they might be important in specific conditions (Fahey et al., 2013). Linear kinetics are also assumed for belowground C-litter for simplicity, considering that this pool represents a rather small portion of the total belowground soil organic carbon. Turn-over times and nutrient composition of belowground and aboveground compartments, and metabolic, structural, and woody litter can vary greatly and are therefore parameterized differently (Kirschbaum & Paul, 2002). This litter pool subdivision maps onto observable litter fractions, because the metabolic component can be regarded as the hot-water extractable litter, while the structural non-lignin and lignin components can be regarded as the acid-soluble (hydrolyzable) and acid-insoluble (unhydrolyzable) fractions, respectively (Campbell et al., 2016; Robertson et al., 2019). Lignin concentration affects decomposition rates (e.g Freschet et al., 2012) and this effect is explicitly accounted for in the model. Note that even though eight distinct C-litter pools are simulated only five pools are physically separated since the distinction within the structural and woody components is only based on the chemical composition. Each pool is thus characterized by a decay coefficient k_i, which determines how fast a given pool is turning over and by a carbon use efficiency CUE_i, assumed temporally constant, which controls the fraction of carbon respired in the process of litter decomposition $(1-CUE_i)$ (Supp. Information).

Total litter respiration and subsurface litter respiration are computed directly from the litter decomposition rate, while the fraction of decomposed litter that is not respired represents the carbon input to the particulate organic carbon (POC) pool.

While there are eight carbon litter pools in T&C-BG, only three litter pools are explicitly tracked for each nutrient (N, P, and K) since the ratio of structural to metabolic carbon/nutrient concentration is prescribed (Kirschbaum & Paul, 2002; Parton et al., 1988) (Supp. Information). The inputs of nitrogen, phosphorus, and potassium to the SOM pool are computed using organic carbon decomposition fluxes and the carbon to nutrient ratio of each pool. During litter decomposition a fraction of nitrogen, phosphorus, and potassium is assumed to leach and directly contribute to the dissolved organic pool or to dissolved minerals in the case of potassium, since we assume that C, N and P are leached in organic form, while K is leached in inorganic form (Sardans & Penuelas, 2015). As a consequence of leaching, organic matter in soils contains a relatively small amount of K. This is reflected in the selection of the leaching coefficients (Supp. Information).

2.1.3 SOC budget

The soil compartments are conceptualized as vertically-lumped with an active zone depth of 25 cm. The C-substrate in the soil is subdivided into particulate organic carbon (POC), mineral-associated organic carbon (MOC) and dissolved organic carbon (DOC), largely following the SOC partition proposed by G. Wang et al. (2013) for the MEND model. The POC fraction is, in turn, separated according to its chemical composition into POC-lignin and POC-cellulose/hemicellulose. This subdivision accounts for the fact that POC-lignin is decomposed by oxidative enzymes (ligninases) produced only by fungi, while POC-cellulose/hemicellulose is decomposed with hydrolytic enzymes (cellulases) produced by both bacteria and fungi (G. Wang et al., 2013; G. Wang, Post, Mayes, Frerichs, & Jagadamma, 2012), leading to different decomposition rates. Physically, POC corresponds to the soil organic carbon associated with particle size $\geq 53\ \mu m$, while MOC refers to the fraction with particle size $< 53\ \mu m$ (e.g., Aoyama, Angers, & N'Dayegamiye, 1999; G. Wang et al., 2013). MOC typically represents the physiochemically protected SOC and its turnover rate can be orders of magnitudes slower than for POC (Conant et al., 2011); DOC is instead immediately available to microbes provided the appropriate en-

vironmental conditions are met. Such representation, however, does not account explicitly for soil aggregates that can provide physical protection to organic matter (Abramoff et al., 2018).

SOC decomposition rates do not depend only on the size of the soil carbon pools but also on the quantity of the extracellular enzymes, which in turn depends on the size and activity of the microbial pools (Schimel & Weintraub, 2003). Modeling enzyme kinetics and microbial pools requires assumptions on the kinetics and knowledge of specific parameters to simulate SOC decomposition, microbial life cycles, and enzyme production, including environmental conditions such as soil temperature and moisture (Manzoni et al., 2016; Schimel, Becerra, & Blankinship, 2017; G. Wang & Post, 2012; G. Wang et al., 2013, 2012). T&C-BG models microorganisms and enzymes explicitly (Lawrence, Neff, & Schimel, 2009; G. Wang et al., 2013) and accounts for four categories of microbial organisms: (i) bacteria, (ii) saprotrophic fungi, (iii) arbuscular mycorrhizae, and (iv) ectomycorrhizae. Arbuscular mycorrhizae (AM), and ectomycorrhizae (EM) can co-exist in some ecosystems, but commonly only one of the two types is present (Brundrett, 2009; Finlay, 2008; Shi et al., 2016), which reduces the number of SOC pools.

Mycorrhizae conversely to bacteria and saprotrophic fungi are unable to feed on DOC and receive their carbon only from the host plant (Baskaran et al., 2017; Finlay, 2008; Johnson, Angelard, Sanders, & Kiers, 2013; Koide, Sharda, Herr, & Malcolm, 2008). However, ectomycorrhizae, differently from arbuscular mycorrhizae, are capable of producing extracellular enzymes, which catalyze SOC degradation and produce DOC, later used by saprotrophic microbes (Lindahl & Tunlid, 2015; Read, Leake, & Perez-Moreno, 2004; Talbot et al., 2013). Extracellular enzymes used for the degradation of POC and MOC produced by bacteria and fungi are separated, for a total of four extracellular enzyme pools. The DOC derived from the depolymerization of SOC due to extracellular enzyme produced by bacteria and fungi is also accounted for separately in two DOC pools. This separation reflects the fact that enzyme production, SOC depolymerization, and DOC acquisition are typically occurring in very localized areas or niches of microbial activity, constrained by the diffusion of resources (Allison, 2005; Tecon & Or, 2017). Such an assumption is also necessary in the model, since the alternative of a unique DOC pool where bacteria and fungi feed over the same substrate did not provide realistic results.

A carbon pool corresponding to soil macrofauna is also explicitly modeled in T&C-BG because macrofauna can consume a non-negligible portion of soil carbon for its metabolism (Chertov et al., 2017; Lubbers et al., 2013; Moore et al., 2004; Osler & Sommerkorn, 2007; Ruiz, Or, & Schymanski, 2015). Soil macrofauna can include different groups, e.g., acari, collembola, enchytraeids, nematoda and earthworms (Fierer, Strickland, Liptzin, Bradford, & Cleveland, 2009) but the overall parameterization of macrofauna in T&C-BG is tailored to endogeic earthworms, because earthworms are representing the largest mass fraction of soil macrofauna. Soil macrofauna is modeled to feed exclusively on POC, because of its higher carbon density when compared to DOC and easier accessibility when compared to MOC. Furthermore, soil macrofuana is assumed to interact only with belowground soil carbon and thus does not affect litter decomposition (it is implicitly included in the first order litter decay parametrization).

The carbon fluxes F_x among the SOC fractions are computed as in the MEND model (G. Wang et al., 2013), using Michaelis-Menten kinetics representing SOC decomposition as the product of extracellular enzymes and substrate mass (POC or MOC) per unit ground area, while microbial carbon assimilation is proportional to microbial biomass and DOC. Both growth and maintenance respiration of microbes are considered (Lawrence et al., 2009; Schimel & Weintraub, 2003; G. Wang et al., 2013). The scheme to quantify growth respiration rates, maintenance respiration rates, enzyme production rates, and microbial mortality rates assumes that maintenance respiration depends on both DOC and microbial biomass, which was found to be theoretically more consistent than other

alternatives (G. Wang & Post, 2012). Mortality coefficients are assumed equal to the respiration maintenance coefficients (Supp. Information).

The production of the four extracellular enzymes is assumed to be proportional to the maintenance respiration and therefore to the size of the microbial biomass pools, while the extracellular enzyme turnover rates are proportional to the size of the enzyme pools themselves. The proportional investment in enzymes is assumed to be the same for ectomycorrhizal and saprotrophic fungi. Differently from G. Wang et al. (2013), we use scaling factors for the enzyme production rate to introduce a non-linear dependence between the microbial biomass and SOC decomposition rates (productivity and respiration of microbes), which has been observed (Sinsabaugh et al., 2014; Zak et al., 1994). Microbial productivity and respiration scale less than linearly with microbial biomass, which suggests the occurrence of larger specific decomposition rates with low biomass or equivalently a saturating effect of microbial activity for large biomass values.

The parameters used to describe SOM biogeochemical reactions are also a function of environmental conditions such as temperature, soil water potential, pH, clay and silt content, and are corrected using specific empirical relations (Supp. Information). Importantly, the fraction of decomposed POC that becomes MOC is assumed to be affected by the availability of reactive surface represented by the clay and silt fractions and on the degree to which this protective capacity is already occupied by organic matter (Six et al., 2002; Stewart, Paustian, et al., 2007; Stewart, Plante, Paustian, Conant, & Six, 2007). Reactive surfaces can become progressively saturated up to the point that there is no space to store additional MOC, and the soil becomes carbon saturated with regards to the MOC fraction (Supp. Information).

The macrofauna assimilation rate of POC is modeled with a linear kinetic, with a kinetic coefficient dependent on soil temperature, effective saturation, clay content, pH, and substrate palatability (Curry, 1998; Ruiz et al., 2015; Whalen, Paustian, & Parmelee, 1999). The total respiration cost of macrofauna is the sum of maintenance and growth respiration. Maintenance respiration is computed using a linear kinetic with a temperature dependence (Whalen et al., 1999) and considering the saturation-dependent level of activity of the macrofauna, i.e., differentiating between resting and active macrofauna (Ruiz et al., 2015). Finally, the macrofauna mortality rate is proportional to the size of the macrofaunal biomass pool (Whalen et al., 1999).

2.1.4 Soil nitrogen, phosphorus and potassium budgets

Soil organic nitrogen dynamics are assumed to follow the carbon fluxes according to the specific carbon to nitrogen ratio C:N of a given donor pool (Kirschbaum & Paul, 2002). The C:N of microbial biomass has been empirically observed to have a low variability and to impose an important stoichiometric constraint (Cleveland & Liptzin, 2007; Manzoni, Trofymow, Jackson, & Porporato, 2010; McGroddy, Daufresne, & Hedin, 2004; Mooshammer, Wanek, Zechmeister-Boltenstern, & Richter., 2014; Mouginot et al., 2014; Xu, Thornton, & Post, 2013). For this reason, target values are prescribed in T&C-BG and nitrogen mineralization or immobilization is modeled to occur whenever the resource C:N is respectively lower or higher than the microbial C:N demand, i.e., biomass C:N divided by microbial CUE. The temporal dynamics of the soil organic matter nitrogen pool, dissolved organic nitrogen, and nitrogen in the macrofuana and microbial biomass pools are explicitly simulated. The temporal dynamics of the inorganic nitrogen pools corresponding to ammonium NH_4^+ and nitrate NO_3^- are also simulated. They depend on net immobilization/mineralization fluxes, nitrogen uptake and leaching, ammonia volatilization, and nitrification and denitrification fluxes, which are simulated with empirical functions of the amount of ammonium and nitrate and environmental conditions (Dickinson et al., 2002). Flux of N from near-surface rocks is not considered, even though it has re-

cently regarded as a significant source of N in mountains and at high-latitudes (Houlton, Morford, & Dahlgren, 2018).

Soil organic phosphorus dynamics are modeled similarly to nitrogen dynamics, with organic phosphorus following the carbon fluxes according to the C:P ratio of each donor pool. As for C:N, the C:P of microbial biomass has been empirically observed to be a relatively constrained quantity in soils (Cleveland & Liptzin, 2007; McGroddy et al., 2004; Mooshammer et al., 2014; Mouginot et al., 2014; Xu et al., 2013), and target values are prescribed in T&C-BG. Phosphorus mineralization or immobilization is simulated to occur whenever the C:P of microbial biomass departs from the target values similarly to nitrogen. The temporal dynamics of the soil organic matter phosphorus pool, dissolved organic phosphorus, and the phosphorus composing microbial biomass pools are explicitly simulated. The temporal dynamics of the inorganic phosphorus pools are simulated following the approach of the CENTURY model (Parton et al., 1988), where the mineral phosphorus represents an undifferentiated sum of PO_4^{3-}, HPO_4^{2-} and $H_2PO_4^{-}$. Other mineral pools represent the amount of phosphorus in the primary minerals, secondary minerals, and occluded phosphorus (Buendia et al., 2010; Parton et al., 1988; Yang et al., 2014; Zhu et al., 2016). The primary mineral source of phosphorus is fed by the tectonic uplift that adds new parent material, while secondary and occluded P minerals are formed through physical and chemical weathering (e.g. Buendia et al., 2010). All these exchanges are regulated through simple linear kinetics (Supp. Information).

Due to its high solubility, a large part of potassium is leached during litter decomposition and the amount of potassium remaining in the organic material is relatively small when compared to the other analyzed nutrients (Sardans & Penuelas, 2015). For this reason and because microbial stoichiometry of potassium is substantially unknown, we do not model potassium content in microbial biomass or macrofuana and only one generic pool of potassium, corresponding to potassium still trapped in the soil organic matter is simulated. Four pools of inorganic potassium in the soil are considered: (i) potassium in the mineral solution, (ii) exchangeable potassium, (iii) non-exchangeable potassium, and (iv) potassium in the primary minerals (Sparks, 1987; Sparks & Huang, 1985). Plant uptake and leaching occur only from the mineral solution pool. Potassium in the solution is in direct contact with the exchangeable phase via adsorption/desorption reactions (Selim, Mansell, & Zelazny, 1976). Furthermore, the flux between non-exchangeable (complex secondary minerals) and exchangeable K, is also governed by linear reactions. Potassium in primary minerals is converted to mineral solution through physical and chemical weathering. Concurrently, the potassium in primary minerals is fed by the tectonic uplift that contributes new parent material and thus primary soil potassium (Supp. Information).

2.1.5 Nutrient leaching, deposition, biological nitrogen fixation and supply of primary minerals

Leaching of nutrients is computed at the bottom of the soil column and it is not tracked further. Leaching is assumed to be proportional to the water leakage rate in $mm\ day^{-1}$ at the soil bottom divided by the total soil water volume in the column in mm times the amount of nutrients in the soil solution (e.g., $gN\ m^{-2}$) (Porporato et al., 2003). This is an approximation, since we are not solving for any nutrient transport process in the soil column and we consider leaching only at the column bottom, even though most of the dissolved nutrients are physically located in the upper part of the soil column in the biogeochemically active zone. However, such an approximation is likely to mostly affect short-temporal dynamics of nutrient leaching (in the order of days) rather than the integrated leaching in the long-term, where an equilibrium between leaching from the biogeochemically active zone and leaching at the soil bottom is expected. See Supp. Information for further details.

Different databases are combined in T&C-BG to provide geographical maps of total (dry and wet) deposition for nitrogen and phosphorus and wet deposition for potassium, which are used as additional inputs to the soil (Supp. Information). Specifically, present-day nitrogen deposition is obtained from Vet et al. (2014), who provide a global one-degree resolution map of wet plus dry deposition of reduced and oxidized nitrogen forms. The pre-industrial nitrogen input is obtained from a global gridded estimate of atmospheric deposition in 1860 (Dentener, 2006; Galloway et al., 2004). Total atmospheric phosphorus deposition maps for current and preindustrial times are obtained from Mahowald et al. (2008). Finally, wet potassium deposition is available for about 480 stations around the world for the period 2005-2007 (Vet et al., 2014). A nearest neighbor interpolation among these values is carried out to obtain an estimate of local potassium deposition as input for T&C-BG.

Symbioses between certain plant species and nitrogen-fixing bacteria represent the major natural source of nitrogen input in some ecosystems (Cleveland et al., 1999; Menge, Levin, & Hedin, 2009). The amount of biologically nitrogen fixed by plants is computed using the same carbon cost of biological nitrogen fixation (BNF) utilized to compute carbon allocation to root nodules (Brzostek et al., 2014) and only when specific plants performing BNF are occurring in a given vegetated patch (Supp. Information).

2.2 Numerical Experiments

2.2.1 Case studies

Hourly meteorological inputs, soil properties and depth, and biome parameterizations were taken from 20 sites corresponding to locations where observations were available to force the model (Table 1) and to analyze the consistency of the results. These sites are representative of all major biomes and cover a wide climatic range, thus allowing quantification of global-scale correlation among key biogeochemical variables. As usual in T&C applications (Fatichi et al., 2016; Fatichi & Pappas, 2017; Mastrotheodoros et al., 2017), biomes were not parameterized with generic plant functional types, but for each site a parameter set able to provide satisfactory results in terms of vegetation productivity, leaf area index, soil moisture, energy and water fluxes, and local phenology was identified acting on the most sensitive parameters. The capability of the original T&C model to reproduce the observed energy and water fluxes and vegetation phenology as well as response to environmental manipulations against observations have been published before for a large number of location worldwide and the 20 selected sites are a subset of those (e.g., Fatichi & Ivanov, 2014; Fatichi et al., 2015; Fatichi & Leuzinger, 2013; Fatichi et al., 2016; Fatichi & Pappas, 2017; Manoli et al., 2018; Mastrotheodoros et al., 2017; Pappas et al., 2016). A single parameter set for the soil biogeochemistry module was selected based on literature parameters and preliminary model tests and is fully documented in the Supp. Information.

2.2.2 Model spin-up and comparison with ecosystem carbon flux observations

Given the lack of detailed knowledge of hourly-scale past climate and changes in land-uses and management practices, for 18 of the 20 locations we use average climatic conditions and average litter inputs to spin-up carbon and nutrient pools running only the soil-biogeochemistry module for 1000 years. Then we further spin-up this initial state simulating once the period for which hourly observations are available with the full T&C-BG. In all simulations, atmospheric CO_2 concentrations were assumed to follow the observed historical trend (Keeling, Piper, Bollenbacher, & Walker, 2009) and nutrient deposition were set to pre-industrial values until 1940 and to current values afterwards for nitrogen and phosphorus (Galloway et al., 2004; Mahowald et al., 2008; Vet et al., 2014). The corresponding conditions in terms of vegetation and soil carbon and nutrient pools

are used as initial conditions for a final simulation from which we compute all quantities reported in the result section as representative of the different locations. The sites are considered to be un-managed with the exception of three grasslands (Chamau, Stubai and TasFACE), where periodic grass cuts are prescribed. In reality, cut grass is removed and the fields are fertilized, however in the model the mowed grass material is left in the field to decompose to avoid removing mass of elements and therefore prescribing fertilizer additions, which are mostly unknown. Only background mortality is assumed for forested sites, assuming no catastrophic events occur.

For two locations only, the University of Michigan Biological Station (UMBS) and Harvard Forest, transient simulations from 1860 to the periods with hourly observations (1999-2014 and 1991-2010, respectively) were carried out to capture forest dynamics after disturbance. Hourly meteorological variables from 1860 to the beginning of the observations were generated stochastically by means of a weather generator (Fatichi, Ivanov, & Caporali, 2011). We imposed disturbances similar to those reported for these ecosystems, specifically, the forest was assumed to be clear-cut in 1923 in the UMBS (Curtis et al., 2002, 2005; Gough et al., 2007; Schmid, Su, Vogel, & Curtis, 2003), and 60% felled down due to wind thrown in 1938 in Harvard (Curtis et al., 2002; Urbanski et al., 2007). Regrowth from seeds (75%) and re-sprouting roots (25%) were assumed for both forests. For these two locations, soil-biogeochemistry C, N, P, K pools before 1860 were obtained from a 1000 year spin-up with average climatic conditions and constant litter inputs as for the others locations but litter inputs were computed with pre-industrial CO_2 levels. Simulations for the observational period in the two transient spin-up cases of the UMBS and Harvard Forest were compared with flux-tower observations of ecosystem respiration and Net Ecosystem Exchange (NEE). Including disturbances at the actual date of occurrence allows a meaningful comparison between observations and simulations, while for all the other locations NEE is expected to be close to zero because of the equilibrium conditions obtained at the end of the spin-up.

2.2.3 Bare-fallow and litter manipulation experiments

For all the 20 locations, a theoretical bare fallow experiment is simulated. The implementation of the bare fallow involved cessation of all litter inputs, root-C exports and nutrient uptakes, allowing the soil carbon and nutrient pools to evolve for 100 years with no inputs, excepts for atmospheric deposition and slow supply of primary minerals through tectonic uplift. Changes in soil organic carbon were then normalized with the initial value and compared with the long-term bare fallow experiments reported by Barré et al. (2010). Additionally, for the location of Harvard forest, the major litter manipulation treatments of the DIRT experimental plots (Bowden et al., 1993; Nadelhoffer et al., 2004; Rousk & Frey, 2015) are modeled to evaluate changes in carbon storage, respiration, and relative dominance of fungi and bacteria. Specifically, we compare the control scenario (CTR) with normal annual aboveground litter inputs, with a double litter (2X, twice the aboveground litter inputs of the control plots) and no aboveground litter (0X, annual aboveground litter inputs excluded) experiments. Simulations refer to the lumped soil-biogeochemistry active zone of T&C-BG (first 25 cm of soil), while observations were carried out separately in the mineral and organic layer of the soil (Rousk & Frey, 2015). Therefore, observations for both mineral and organic soils are reported in the result section for comparison. Simulations are averaged over a period of three years after 16 years of imposed treatment, while observations represent snapshot differences observed after 23 years of treatment. This discrepancy depends on meteorological variables that were available only for 19 years to run the model.

2.2.4 Nitrogen fertilization

A numerical nitrogen addition experiment was carried out for Little Prospect Hill (LPH), MA, USA, still comprised within the Harvard forest long-term ecological research

area, where a nitrogen addition experiment (Frey et al., 2014; Magill et al., 2004; Tonitto, Goodale, Weiss, Frey, & Ollinger, 2014) and long-term observations (15 years) of nitrogen fertilization on pine and hardowood sites were carried out. Since the pine forest showed decreasing productivity in response to N-addition due to soil-acidity (not implemented in the model), we only compare the response for the hardwood site as done by previous modeling studies (Meyerholt & Zaehle, 2015). Two levels of nitrogen addition (5 and 15 $gN\,m^{-2}\,year^{-1}$) were given as input in six different applications separated by 30 days during the growing season as in Magill et al. (2004). We test the model response in terms of changes in leaf-nitrogen content. Beyond the actual applied treatments, other levels corresponding to 1, 3, 10, 30, and 100 $gN\,m^{-2}\,year^{-1}$ were used in numerical experiments. These treatments, while unrealistic, are used to evaluate the model capability to reproduce the responses of forest N cycling to continuing N addition, e.g., N saturation, as hypothesised by Aber et al. (1998); Aber, Nadelhoffer, Steudler, and Melillo (1989) and synthesized by Niu et al. (2016). In order to generate some nutrient limitation rather than arriving to the long-term equilibrium that is obtained after the spin-up described before, soil organic nitrogen is reduced of 5% in comparison to the value obtained at equilibrium. Such a small adjustment allows introducing nitrogen limitation and simulating an N-addition stimulation of NPP as observed in the field.

3 Results

3.1 Local comparison of carbon fluxes with flux tower data

Fully transient simulations for the UMBS site show that T&C-BG is able to capture the main variability of ecosystem respiration (RE) and Net Ecosystem Exchange (NEE) at daily and monthly scale, with a coefficient of determination (R^2) equal to 0.92 and 0.93 for NEE and RE at monthly scale and R^2 of 0.67 and 0.84 at daily scale for NEE and RE, respectively (Fig. 1). Despite the overall good correlation, simulations tend to overestimate ecosystem respiration during summer months and slightly underestimate respiration during the autumn, which leads to carbon sink conditions (negative NEE), while observations have positive NEE values during October. Performance is slightly worse (R^2 of 0.84 and 0.67 at monthly scale and 0.57 and 0.55 at daily scale for NEE and RE) for Harvard forest where variability of observed carbon fluxes is larger than simulated, and primarily the consistent negative trend in observed NEE (Keenan et al., 2013; Urbanski et al., 2007), is not as evident in the simulations (Fig. S2). For both sites the average carbon sink, which is related to the recovery from historical disturbances and partially also to CO_2 fertilization, is reproduced by the model but with a lower magnitude (Table 2). Other carbon and nitrogen fluxes and states that can be compared at UMBS are the aboveground standing biomass and total SOC. Aboveground biomass is slightly underestimated by the model, which may be expected given the simplified description of the 1923 forest disturbance. SOC observations are rather uncertain (Gough, Vogel, Schmid, & Curtis, 2008; McFarlane et al., 2013) ranging from 5.5 to 8 $kgC\,m^{-2}$ with simulations that are closer to the lower estimate. Nitrogen-mineralization rates are similar to local observations (Table 2) and are comparable to what would be expected for the productivity of UMBS ($ANPP = 776\ g\,DM\ m^{-2}\ year^{-1}$), when compared to a review of the net N mineralization - Aboveground Net Primary Production (ANPP) relation in conifer and hardwood forests in the mid-west USA (Reich, Grigal, Aber, & Gower, 1997). Nitrogen leaching and gaseous N-efflux are an order of magnitude smaller than N-mineralization. While gaseous efflux is similar in model simulations and observations, there is almost an order of magnitude difference in NO_3^- leaching which is overestimated by the model.

3.2 Global scale patterns of carbon cycle components

A few studies have quantified the global-scale relation among Net Primary Production (NPP), litterfall, SOC, soil respiration, nutrient mineralization rates, microbial and macrofauna biomass (Fierer et al., 2009; Gill & Finzi, 2016; Raich & Nadelhoffer, 1989; Xu et al., 2013; Zak et al., 1994). Here, we compare these variables for the 20 modeled sites with the values published in literature. These comparisons are meant to demonstrate the model ability to reproduce broad-scale patterns as emergent features of the simulations rather than matching values at specific locations. Raich and Nadelhoffer (1989) found a strong correlation between soil respiration and litterfall in global forests, a correlation that is very well reproduced by the model simulations (Fig. 2a). Simulations across the 20 sites spanning different climates and biomes are also consistent with observed global patterns in belowground communities published by Fierer et al. (2009). The relation between total microbial biomass and vegetation productivity is well represented for both total NPP and belowground NPP (Fig. 2b,c). Soil respiration increases almost linearly with microbial biomass, with a tendency for microbial biomass to saturate at high-productivity/respiration sites (Fig. 2e). Total SOC for a given microbial biomass is underestimated when compared to values of Fierer et al. (2009). This can be the result of model limitations in considering only 25 cm of lumped soil-biogeochemistry active zone. Observations cover the first meter of soil and if microbial biomass and SOC have different depth profiles (Xu et al., 2013) a mismatch has to be expected comparing different integrated depths. Macrofaunal biomass is simulated to be in the range of 0 to 4.6 $g\,C\,m^{-2}$, which is similar to the range reported by Fierer et al. (2009) and increases proportionally with microbial biomass and therefore site productivity, even though simulated macrofaunal biomass is a bit underestimated for a given microbial biomass (Fig. 2f).

Patterns of nitrogen and phosphorus mineralization in relation to Gross Primary Production (GPP) have been recently assessed by Gill and Finzi (2016). Simulations in the 20 sites are typically consistent with those values, although simulated nutrient mineralization rates tend to be slightly larger than observed for intermediate values of GPP (Fig. 3a,b). Modeled nutrient mineralization rates are very high for two alpine grasslands but they are plausible given the high productivity and relatively large nutrient content of grass leaves and the fact that grass litter is left on the field in the simulations. Nitrogen Use Efficiency (NUE) and Phosphorus Use Efficiency (PUE) computed as the ratio of GPP to nutrient uptake rates have the same magnitude of the values published by Gill and Finzi (2016) even though simulated NUE is generally smaller. Simulated values are rather scattered and do not follow the pattern of increase in PUE and decrease in NUE with GPP from high-latitude boreal ecosystems to low-latitude tropical forests (Fig. 3c,d). However, deserts and semi-arid locations were not analyzed by Gill and Finzi (2016), and therefore the comparison is forcefully limited.

3.3 SOC pools and nutrients

Since the model simulates various functional SOC pools, it is possible to evaluate their relative magnitude (Fig. 4). With the selected parameterizion, the mineral associated carbon (MOC) pool is the largest fraction of SOC and spans between 58 and 79% of SOC, depending on the ecosystem, with a mean MOC:POC of 2.8. This is supported by a few observations collected in grasslands and agro-ecosystems (Cambardella & Elliott, 1992; Sherrod, Peterson, Westfall, & Ahuja, 2005) and by the recent observations of MOC and POC fractions in a selected subsample of the LUCAS dataset of European soils (Robertson et al., 2019). The plausibility of the simulated values is confirmed by the comparison of the MOC concentration with observations reported in Six et al. (2002) (Fig. 5b). Mineral associated carbon tends to decrease with decreasing silt plus clay fraction in both simulations and observations, because the physical surfaces in the soil starts to saturate earlier with MOC for coarser soil textures (see Supp. Material). POC-Cellulose

is on average smaller than POC-Lignin (11% versus 16% of SOC) since it is consumed faster, but POC-Lignin has a much larger variability across ecosystems, which is related to the composition of the litter with grasslands having a much smaller fraction of POC-Lignin when compared to forests or shrubs. Microbial biomass is simulated to be on the range 1.0-3.1% of SOC (Fig. 4b) consistent with observations published in several articles (G. Wang et al., 2013; Xu et al., 2017, 2014, 2013). However, the microbial nitrogen and phosphorus fraction of SOM tend to be underestimated at low values of NPP (Fig. S3). DOC is typically a very small fraction, less than 2% of SOC (Fig. 4c), as supported from observations (G. Wang et al., 2013). DOC mass is in the same order of magnitude as microbial biomass (Fig. 4d), and generally smaller for high-productivity sites (15% of microbial biomass) and larger for low-productivity sites (80%-100% of microbial biomass). Enzyme C-pools are not shown but their sum is on the order of $0.1-0.4$ $g\,C\ m^{-2}$ and account for less than 0.005% of SOC (no empirical evidence is available to test this prediction). The average simulated mass ratios between fungi and bacteria is 7.0 (Fig. 4e). The magnitude is supported by a collection of observations of fungal to bacterial phospholipid fatty acid (PFLA) ratios that once converted to C biomass ratios provide an average of 6.0 (Waring, Averill, & Hawkes, 2013). However, the simulated variability is smaller than observations and mostly due to the modeled variability in mycorrhizal biomass. A few additional observations support the fact that fungi have larger biomass than bacteria (Joergensen & Wichern, 2008; Six, Frey, Thiet, & Batten, 2006), e.g., at least 4-5 times larger (Ananyeva, Castaldi, Stolnikova, Kudeyarov, & Valentini, 2015). Bacteria have a faster metabolism (productivity and respiration rates) and therefore their biomass is typically smaller. The emergent ratio between saprotrophic and mycorrhizal fungi from the simulation is 1.5. This is a poorly known and largely unconstrained quantity, and few indications for boreal ecosystems tend to support a ratio around or less than 1 (Bååth, Nilsson, Göransson, & Wallander, 2004; Clemmensen et al., 2013).

SOM nutrient content ranges in terms of C:N and C:P on a mass-basis are 9-15 and 60-79, respectively (Fig. 5a), well within the range of global observations (Cleveland & Liptzin, 2007; Mooshammer et al., 2014), even though the simulated variability across biomes may be smaller than what typically observed (Xu et al., 2013). This is probably the result of having a constrained range of nutrient contents in plant tissues across ecosystems (e.g., N:P does not vary) and fixed microbial C:N and C:P ratios. C:N, C:P, and C:K values of leaf-fall and reproductive-fall litter are indeed well within the range of observed variability (Holland et al., 2014), but the 20 analyzed locations span a much lower range than observations (Fig. S4). The C:N and C:P ratios are also well within the observed range of woody and leaf litter chemistry composition (data summarized in Manzoni et al. (2017)), and not surprisingly of soil microbial biomass (Fig. 5a). However, in such a case the C:N and C:P ratios are prescribed for each microbial community and the limited differences among sites are only dictated by variability in the proportion among bacteria, saprotrophic, and mycorrhizal fungi. While observations show higher variability for all these quantities, the magnitude of the decrease in C:N and C:P from litter, soil organic matter, to soil microbial biomass is correctly captured by the model.

3.4 Microbial activity, root-C export, and soil respiration partition

Microbial productivity and respiration have been shown to scale linearly with microbial biomass (Sinsabaugh, Shah, Findlay, Kuehn, & Moorhead, 2015). This is expected also from T&C-BG model construction and is indeed confirmed across ecosystems (Fig. S5). The slope of these relations in a log-log plot has been postulated to be less than 1, specifically slopes of 0.7-0.8 have been shown for production versus biomass, and slopes of 0.5 for respiration versus biomass (Sinsabaugh et al., 2015), suggesting a less efficient use of resources at higher biomass. Slopes computed from simulations are 0.93 and 0.94 for bacteria and fungi respectively, and for production versus biomass and respiration versus biomass. While the same slope for production and respiration is expected from

model construction, the similarity between bacteria and fungi emerges from simulations. Results suggest that while there is a lower efficiency at higher biomass rates, introduced in the model through the variable allocation to extracellular enzymes, this is probably not sufficient to capture the observed lower-than-one slopes, even though uncertainties in observations are also very large (Sinsabaugh et al., 2015).

Other simulated global patterns are shown to describe the model behavior and plausible magnitude of quantities that are typically difficult to measure (Fig. 6). SOC tends to increase with carbon input of litter, especially for carbon inputs lower than 500 $g\,C\,m^{-2}\,year^{-1}$. However, there is a very large variability of SOC at high carbon inputs, which highlights how standing carbon pool is a complex integrated variable only loosely correlated with C-inputs. SOC increases slower at high litter inputs, as is also the case in the relation between SOC and abovground NPP (a proxy of litterfall) across ecosystems (Zak et al., 1994). Note, however, that we do not simulate any peatland soil, where very high carbon stocks may be expected also for small inputs. Microbial respiration for unit of microbial biomass, typically named Microbial Metabolic Quotient, MMQ (Xu et al., 2017), tends to be larger with low microbial pools, since microbes are assumed to be more efficient in allocating carbon to enzyme as their biomass decreases (Fig. 6b). Simulated differences in MMQ for high and low microbial biomasses are less than 50%, smaller than reported by previous studies (Averill, Waring, & Hawkes, 2016; Zak et al., 1994). However a recent global analysis of MMQs shows a less clear pattern of increasing MMQ with decreasing microbial biomass (Xu et al., 2017). The simulated average microbial metabolic quotient is 0.32 $mgC\ \ gC^{-1}\ \ hour^{-1}$, a value five times smaller than published by Xu et al. (2017), but our estimate is reasonable because both microbial biomass and total respiration are well captured (Fig. 2). The discrepancy can be originated by observations, which are typically derived from short-term laboratory studies of soil samples collected from superficial layers and disturbed prior to incubation, whereas simulated values represent long-term integrated MMQ at ecosystem scale.

Root carbon exudation computed from simulations appears to be a relatively small fraction of NPP (0.6-4.9%), typically less than 2% (Fig. 6c). Carbon export to mycorrhiza instead is a more considerable component that averages around 11.3% of NPP, with larger values (around 20-25%) for low productivity drier sites and decrease to 4-7% for wetter sites (Fig. 6d), with the latter values supported by field estimates (Brzostek, Greco, Drake, & Finzi, 2013; McCarthy et al., 2010). Even though mycorrhizal biomass is smaller in low-productivity regions, the simulated plant cost for its maintenance decreases less than proportionally to the decrease in NPP, because nutrient availability decreases strongly in these dry ecosystems, which leads to the behavior observed in Fig. 6d. Mycorrhizal biomass observations in arid and semi-arid sites are absent or rare, and therefore the confidence in such a result is minimal (shaded area) since it is difficult to test if this model result is realistic or driven by the imposed model structure and unique parameterization adopted for all sites.

Simulations also allow to shed light on the relative contributions to respiration, partitioning it among fine-roots, bacteria, fungi and macrofauna. There is a noticeable site-to-site variability with fine root, fungal, bacteria and macrofaunal respiration accounting on average for 33% (18-54), 40% (29-49), 24% (14-30) and 3% (0-9) of total belowground respiration, with absolute ranges given in parenthesis (Fig. 7). Fungal respiration can be further subdivided in mycorrhizal fungi respiration, which is on average 5% (2-12) and saprotrophic fungi respiration, which is on average 35% (21-46). A mycorrhizal fungi respiration contribution of 2-12% to total soil respiration is well supported by few available observations (Fenn, Malhi, & Morecroft, 2010; Moyano, Kutsch, & Rebmann, 2008; Nottingham, Turner, Winter, van der Heijden, & Tanner, 2010; Tomè et al., 2016). Based on these simulations, the ratio between soil heterotrophic respiration and total soil respiration is 0.67±0.08, which is very close to the 0.63±0.16 ratio reported in the updated global soil respiration database for the 2007-2014 period (Bond-Lamberty,

Bailey, Chen, Gough, & Vargas, 2018). Macrofaunal contribution increases with NPP, not surprisingly since macrofauna (mostly earthworm) activity is largely suppressed or eliminated because of soil moisture limitations in semi-arid sites. The fine root contribution is quite variable but tends to decrease at large NPP, where fine-root biomass represents a smaller fraction of living plant tissues, when compared to sites with lower NPP. Such a decrease in root respiration contribution is accompanied by an increasing contribution of bacteria, which is less variable across sites than the other components. Fungal respiration, which includes saprotrophic and mycorrhizal contributions, is the largest component of soil respiration, even though the ratio of fungal to bacterial respiration is much smaller than their biomass ratio (Fig. 4). This is the result of a faster bacterial metabolism, as observed in empirical studies (Sinsabaugh et al., 2015; Waring et al., 2013), and reflected in the model parameterization (Supp. Information).

3.5 Bare fallow experiment

Changes in relative SOC with time after cessation of litter inputs were in good agreement with the range of variability found in the seven experiments located in humid climates reported by Barré et al. (2010)(Fig. 8a). In this virtual experiment, we considered only locations with precipitation above 700 $mm\,year^{-1}$ consistent with the climate of the experimental sites. Simulating drier conditions lead instead to slower SOC decay, especially after 50-60 years (Fig. S6). Model simulations can be used to look at the behavior of the different soil organic matter pools with time after input cessation (Fig. 8b to g). Bacteria and saptrotrophic fungi tend to lose relatively quickly 50% of the their biomass but they persist in most locations after 100 years with saprotrophic fungi having slightly higher remaining fractions. Mycorrhizal fungi, not surprisingly, survive only few years after all litter and C-export inputs are stopped because they are not supported anymore by the host plant and they cannot feed on DOC. The predicted faster decrease of microbial biomass compared to total SOC is supported by observations from three long-term experiments including a bare fallow (G.-H. Wang et al., 2009; Witter & Kanal, 1998; Yu et al., 2013). In fact, in these experiments microbial biomass C in the topsoil scales as total SOC to the power 1.6 ($R^2 = 0.88$). Relative respiration follows temporal dynamics similar to the biomass of bacteria and saprotrophic fungi, with respiration representing only 50% of the initial one after 3-8 years and generally less than 20% after 50 years. SOM C:N and C:P ratios decrease through-time showing a relative accumulation of nutrients with respect to carbon but the spread among locations is significant with C:N and C:P ranging from 0.6 to 0.8 of their initial values after 100 years. In the simulations, there is a negative correlation between the initial amount of SOC and the remaining SOC after 100 years of experiments, which supports the idea that removing litter input where input is limited has a lower effect on SOC and that it is more difficult to lose carbon from already carbon-poor soil when compared to carbon rich soils (Fig. 8h).

3.6 Litter manipulation experiment

Simulations corresponding to the litter manipulation experiment DIRT are compared with observations (Fig. 9). In order to avoid comparing absolute numbers, which would be difficult and uncertain at the ecosystem scale, we normalized the observed values to the simulated control scenario (no treatment) so that modeled and observed control scenario values forcefully overlap in the Figure 9. This allows to only compare the relative magnitude of the treatment effects in the simulations and observations. Treatment effects for observations were reported for both organic and mineral soil layers that are not distinguished in the model. Simulations are therefore expected to lay between these values or close when the model results are realistic. The responses to litter doubling (2x) in terms of increases in soil organic carbon, C:N, soil respiration and relatively stable ammonium in soil are captured by the model given potential uncertainties in the

observations (Fig. 9). However, the response to litter exclusion (Ox) is weaker in the model than in reality for SOC but well represented for the other quantities. Simulated saprotrophic fungi and bacteria productivity increases with litter addition and decreases with litter exclusion, with the simulated ratio fungi to bacteria increasing slightly with decreasing litter quality (Ox), and decreasing otherwise (2x). This trend is not observed in reality where fungal productivity decreases in the 2x − CTR − Ox transition but bacterial productivity does not (Rousk & Frey, 2015), suggesting that mechanisms more complex than those implemented in the model may be at play.

3.7 N-addition experiment

Results of the numerical nitrogen addition experiment for Little Prospect Hill (LPH) are compared with observations of foliage N concentration and relative change in NPP for the hardwood biome (Fig. 10) and against expectations of response patterns of forest N cycling to continuing N addition (Aber et al., 1998, 1989; Niu et al., 2016). Foliage N concentration and NPP increase with N addition but at relatively slow rates, partially due to the stoichiometric buffer offered by nutrient storage in the model and to the smooth response of photosynthesis and respiration to increased N-concentrations. Even with 15 $gN\,m^{-2}\,yr^{-1}$ of nitrogen addition, NPP increases by 19% and the relative N concentration is 1.60 times larger than under control conditions. Most important, NPP and foliage N concentration remain realistic also for extremely high fertilization rates (30, 100 $gN\,m^{-2}\,yr^{-1}$) (Fig. 10). Net N mineralization, which is computed as the difference between N-mineralization and immobilization rates, increases with N-addition, except for very high values of N-addition, at which simulated N chemical immobilization following N-applications more than compensates for the increase in mineralization rates. N leaching, gaseous emission and standing ammonium and nitrate pools increase almost linearly (less than 3 times) for N addition rates up to 5 $gN\,m^{-2}\,year^{-1}$ but they grow exponentially for larger fertilization rates, being more than 80 times larger for N addition of 30 $gN\,m^{-2}\,yr^{-1}$. This exponential growth suggests that N-saturation is simulated at such high fertilization rates for this ecosystem. The overall response is very much consistent with the N-saturation hypothesis described in Niu et al. (2016), where competing mechanisms (plant N uptake, denitrification, N-leaching, microbial N demand) are concurrently at play for relatively low soil N available, but where losses dominate as soon as N availability exceeds a given threshold.

4 Discussion

4.1 Model structure and functionality

Soil biogeochemical dynamic processes were represented along with the corresponding vegetation and climatic context by combining a detailed soil-biogeochemistry module with an existing ecosystem/land-surface model, T&C. The soil-biogeochemistry module explicitly represents SOC functional pools, including extracellular enzymes and separates microbial biomass in bacteria, saprotrophic and mycorrhizal fungi. Biogeochemical processes are affected by water, energy, and vegetation dynamics above and belowground, and in turn they affect vegetation structure and behavior through plant mineral nutrition. Twenty locations were selected as representative of different climates and biomes and because they corresponded to specific manipulation experiments. This study is among the first to compare model predictions of detailed soil biogeochemical processes with a range of plot-scale observations across multiple ecosystems leading to a number of important considerations.

Only a few observations are available to directly test microbial explicit models. Moreover, while for some quantities there is abundance of data (e.g., soil C:N and C:P ratios), for others it is difficult to even simply assess if the order of magnitude of the predictions is correct (Fig. 6). Scarcity of quantitative data to evaluate mechanistic soil-biogeochemistry

models necessitate the use of innovative ways to check the plausibility of simulations and overall the model behavior. In this study, we rely on observations of global patterns in belowground communities, mineralization rates, scaling relations among biomass and respiration, and ratios between soil organic carbon components. The latter are considered particularly useful to evaluate model realism because several ratios (e.g., microbial biomass to SOC, or DOC:SOC) are known and have a relatively constrained variability. Furthermore, we use observations of effect size from manipulation experiments (bare fallow, litter addition and subtraction, N-fertilization). These are compared in relative sense, since it is difficult to scale the observed column scale quantities into an ecosystem quantity in absolute terms. However, already capturing direction and magnitude of changes induced by the manipulation is an important test for the model.

Global relations among microbial biomass, litterfall, soil respiration, NPP, SOC, macrofauna biomass and mineralization rates are mostly captured by T&C-BG (Fig. 2 and 3), with a very realistic and constrained range of microbial biomass to SOC ratio (1.0-3.1%), DOC to SOC ratio, and fungi to bacteria biomass ratio (Fig. 4 and 5). These values are supported by published estimates (Anderson & Domsch, 1989; Fierer et al., 2009; Serna-Chavez, Fierer, & van Bodegom, 2013; G. Wang et al., 2013; Wardle, 1992; Waring et al., 2013; Xu et al., 2014, 2013; Zak et al., 1994). The model results are encouraging considering the single parameter set used across all locations (e.g., absence of local tuning). It suggests that vegetation (via litter production) and climate control these patterns and that global-scale soil-biogeochemical dynamics can be captured despite large uncertainties in the parameter values. However, these uncertainties should be explored in the future, as soon as additional observations to estimate parameters and further test the model will be available. Because of the use of generic parameterizations, predictions are likely to downgrade significantly when reproduction of a specific quantity (e.g., SOC in a given location) and local dynamics are sought. Therefore, caution should be adopted for local model applications.

4.2 Evaluating mechanistic soil biogeochemical models - data scarcity and ways forward

For more detailed analyses and use of mechanistic models in a predictive mode, there is a price to pay - namely the determination of the uncertainty range of a very large number of parameters. Modeling experience and detailed sensitivity analyses can help identifying the most influential parameters and their effects on certain processes (Pappas, Fatichi, Leuzinger, Wolf, & Burlando, 2013). Hopefully, studies like this one will inspire and guide future publication of biogeochemical pool sizes and fluxes and microbial traits that correspond or are closely related to model parameters (e.g., Allison, 2017; Robertson et al., 2019; Sinsabaugh et al., 2014, 2015; G. Wang et al., 2013). However, care must be taken in comparing ecosystem scale estimates with meta-analyses of laboratory samples, such as in the case of differences in microbial metabolic quotient between simulations and observations (Xu et al., 2017). Some of the parameters are not even measurable directly and must be inferred from the response of time variable fluxes or pools (e.g., carbon allocation to extracellular enzymes). An alternative option is to use mechanistic individual-based models that consider physiological and biophysical properties of microbes (Schimel & Weintraub, 2003) and detailed transport processes in soil pore networks (Ebrahimi & Or, 2016, 2017; Long & Or, 2005) to quantify some of the microbial physiological parameters (e.g., uptake rate of DOC for unit of microbe) required by ecosystem-scale models such as T&C-BG. A larger amount of information on parameters will allow in the future to characterize variability of microbial traits (Allison, 2012), at least broadly as it is currently done for vegetation properties (Bonan et al., 2011; Bonan, Levis, Kergoat, & Oleson, 2002; Pappas et al., 2016); see also discussion in Wieder, Allison, et al. (2015). While parameter identification and uncertainty represents a considerable shortcoming of the presented approach, in a well-tested model a number of constraints imposed by conservation of mass, stoichiometric relations, and generally the mechanistic

nature of the model can, arguably, prevent unrealistic and implausible outcomes for future environmental conditions. These predictions could be equally or more plausible than extrapolation of data-driven approaches, especially, because data-driven approaches are uncertain beyond the range of observations.

Detailed observations of multiple carbon and nutrient fluxes and states in a single location will be also very important for a more rigorous test of some of the mechanistic implementations of the model. Since most of the simulated variables correspond to measurable quantities, data to model comparison should be more straightforward than it is currently in traditional soil-carbon models that use fast and slow C-pools (e.g., Krinner et al., 2005; Sitch et al., 2003). Additionally, reproducing realistic local conditions e.g., SOC and NEE (Fig. 1) or N-fertilization effects require a detailed knowledge not only of the current conditions, but also of the history of disturbances and land-use changes to carry out a meaningful data to model comparison. A simple discrepancy in modeled and observed total SOC, a frequently made evaluation in Earth System Models, has probably little value if the model spin-up does not correspond to the local history.

This work is among the first to compare certain modeled quantities to observations, such as the biomass ratio between fungi and bacteria or mycorrhiza and saprotrophic fungi, MOC and POC values, or the NPP fractions of root C-exudation and allocation to mycorrhizae. While a few references seem to support their plausibility (Brzostek et al., 2013; Ekblad et al., 2013; Hobbie, 2006; M. N. Högberg & Högberg, 2002; Moyano et al., 2008), additional checks are required in the future. Among the important quantities that are difficult to observe there is the relative contribution of fine root, fungal, bacteria and macrofauna to total belowground respiration, which have been found to be 33, 40, 24, and 3% on average, of the 40% fungal respiration, 5% is attributed to mycorrhizal fungi and the remaining 35% to saprotrophic fungi (Fig. 7). The simulated ratio between soil heterotrophic respiration and total soil respiration (0.67 ± 0.08) is well supported by recent observations (Bond-Lamberty et al., 2018). Thus, results confirm that autotrophic fine root respiration is a significant component of soil respiration (P. Högberg et al., 2001) and suggest that bacteria and fungi may contribute similarly to soil organic matter turnover and therefore respiration fluxes despite considerable different biomasses. While belowground macrofauna contribution is generally small, there are wet locations where it cannot be neglected ($\sim$ 9%). The above quantities are dependent on the selected parameterization and difficult to test thoroughly; however, the mechanistic nature of the model and the overall correct representation of total respiration fluxes and carbon pool patterns suggest that they are realistic.

4.3 Current model strengths and limitations

Results in reproducing long-term bare fallow experiments are encouraging considering that there is no calibration involved and the complexity of the model (Fig. 8). In this regard, an important finding is the necessity of an increased allocation to enzyme production as microbial biomass decreases in order to correctly reproduce the SOC decay with time. Without such a distinctive model solution, T&C-BG overestimates SOC in bare-fallow experiments, because microbial biomass depletes the available DOC after few years, impairing decomposition (Fig. S6b). An increasing enzyme production rate per unit of microbial biomass with decreasing substrate (or other adjustments Georgiou, Abramoff, Harte, Riley, and Torn (2017)) emerges as a fundamental feature for microbial and enzyme explicit soil models. This solution has not been implemented in the original MEND model (G. Wang et al., 2013) neither in many of the microbial explicit models, which therefore can likely fail the bare-fallow test. In an analogous way, introducing a dependence between capability of a soil to store MOC and availability of physical surfaces (summarized as silt plus clay fraction) allows the model to reproduce a realistic MOC content (Fig. 5) and saturation of MOC with increasing C litter input (Stewart, Plante, et al., 2007), which would not be obtained otherwise. Despite such features,

microbial metabolic quotient increases only slightly with decreasing NPP (Fig. 6) as supported by recent observations (Xu et al., 2017), but in contrast to others that show a much stronger increase (Zak et al., 1994). Most important, the scaling of microbial productivity/respiration versus biomass is overestimated by the model (Fig. S5). This underlines that CUEs should be more variable than what currently assumed in T&C-BG, which is using constant values, and probably dependent on the microbial biomass and not only on the substrate characteristics. It also emerges that the target plant tissue stoichiometry for the different locations, which are all assumed to be related to leaf-nutrient content, are less variable than in reality, as reflected in a limited range of C:N and C:P ratios in litter-fall and SOM and in lack of specific patterns in NUE and PUE across productivity gradients (Fig. 5, 3 and Fig. S4). For instance, the N:P ratio is currently constant in T&C-BG across sites and biomes, while it has been shown to depend on latitude and temperature (Reich & Oleksyn, 2004). The comparison with the litter manipulation experiment is satisfactory (Fig. 9), but there are specific patterns, e.g., in the fungal-to-bacterial productivity ratio, which are not reproduced by the model, especially for litter exclusion, underlying that more complex dynamics can indeed occur.

The model simulated response to N-fertilization seems to be consistent with expectations (Fig. 10) and few available observations (Magill et al., 2004; Niu et al., 2016), which points to a relatively robust model structure in handling fertilization responses. This is partially the result of modeling solutions that realistically buffer the consequences of nutrient changes, e.g., plant nutrient storages and stoichiometric flexibility. The obtained dampened photosynthesis/respiration response to changes in tissue nutrient concentration is also an important and realistic model result. Nonetheless, there are responses such as the general trend toward a decline in abundance of microbes and mycorrhizae following N-addition (Treseder, 2008; Wallenstein, McNulty, Fernandez, Boggs, & Schlesinger, 2006), that are not currently simulated by the model. Therefore, additional tests to evaluate and refine the role of mycorrhizae and the nutrient cycles in the model are necessary, including P and K dynamics, which are rather empirical and not tested in this article. These tests will allow to draw more definitive conclusions on the realism of simulations describing changes in nutrient availability and interactions with microbial dynamics.

5 Conclusions

A novel soil-biogeochemistry module with a mechanistic representation of soil organic matter decomposition and microbial activity and diversity has been combined with an existing land-surface and vegetation model. Results are realistic in reproducing large scale patterns in a number of relations involving microbial biomass, NPP, SOC, mineralization rates, macrofauna biomass, and SOC components as well as major response to important manipulation experiments, such as bare fallow, litter addition and subtraction, and N-addition. However, considerable local differences (e.g., simulated NEE at UMBS and Harvard forests) and incapability to reproduce specific patterns e.g., the decline in microbe following N-addition or the latitudinal gradients of PUE and NUE suggest that there is room for model refinement. Expectations in matching exactly local quantities, as observed profile-scale SOC, should be also low, with the generic parameterization adopted in this study. Many quantities or ratios among SOC components have been presented for one of the first time and require benchmarks with other modeling studies and validation with new or unpublished measurements. This reinforces the quest for quantitative observations (e.g., $g\,C\,m^{-2}$) useful to test such a type of models. Despite limited data validation and parameter uncertainty, it is fundamental to show the capabilities and potentials of detailed mechanistic models of soil biogeochemistry to capture patterns observed across ecosystems and in manipulative experiments, with the ultimate scope of improving projections of the future water, carbon, and element cycles. The use of such a modeling approach in conducting virtual experiments, where effects of changes in en-

vironmental variables on soil microbial dynamics, carbon storage, plant growth, can be extensively analyzed represents a fundamental approach for a better quantification of soil and ecosystem services in a changing environment.

1054 # Figures

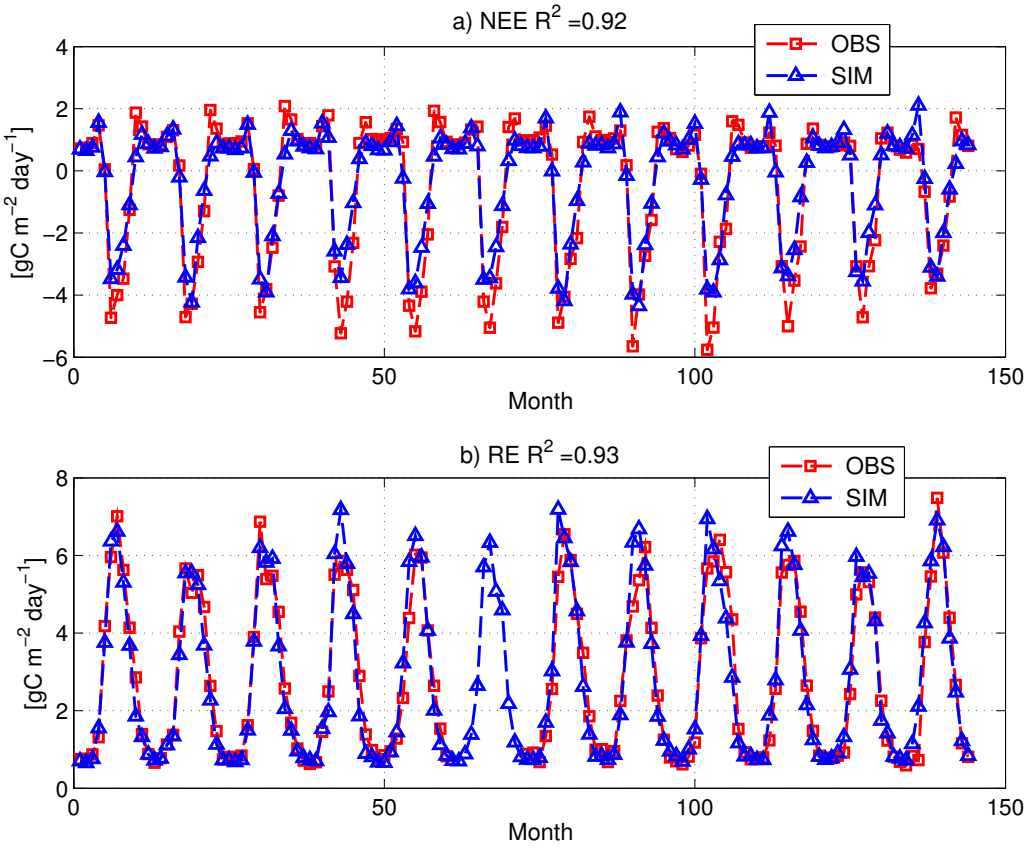

Figure 1. A comparison between the monthly observed (OBS) and simulated (SIM) (a) Net Ecosystem Exchange (NEE) and (b) ecosystem respiration (RE) for the UMBS site.

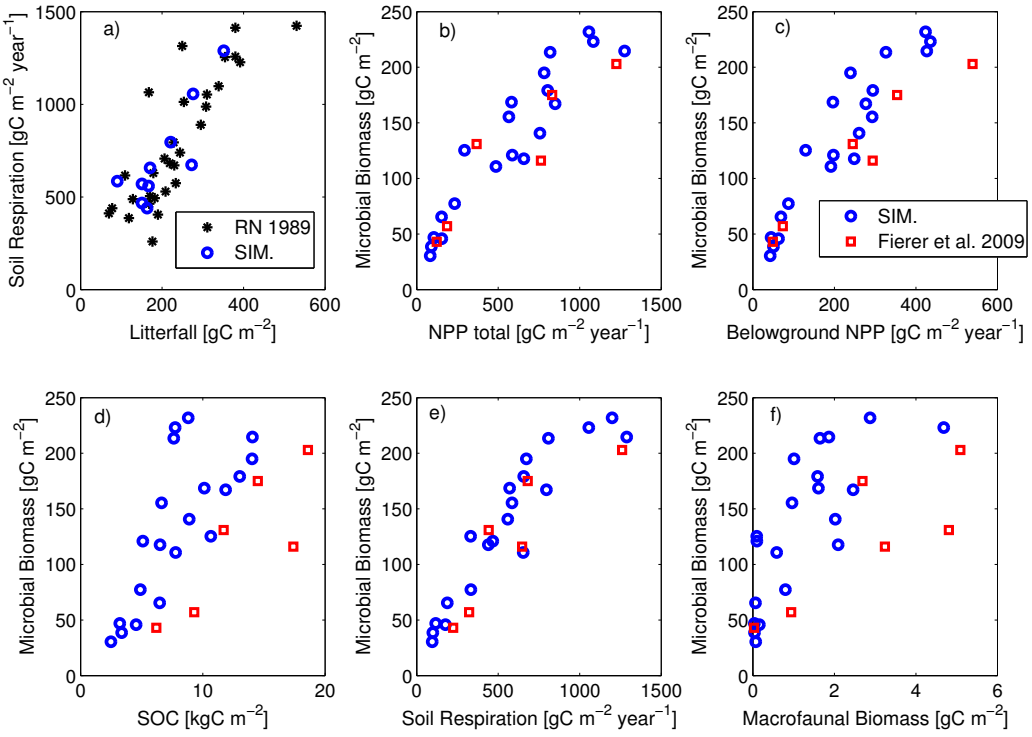

Figure 2. (a) Scatter plot between soil respiration and litterfall in forested ecosystems, blue circles are simulations and black points are observations from the sites considered reliable in Raich and Nadelhoffer (1989). Simulations are only shown for forested sites for consistency with observations and simulated litterfall includes only leaves. Scatter plots between microbial biomass and (b) total Net Primary Production (NPP), (c) belowground Net Primary Production, (d) soil organic carbon (SOC), (e) soil respiration, and (f) macrofaunal biomass. Circles are the time averaged simulated value for the 20 analyzed locations, the red squares correspond to the values reported in Fierer et al. (2009), which are representative of different biomes globally. The Tundra biome is excluded because there are no tundra sites among the simulated locations.

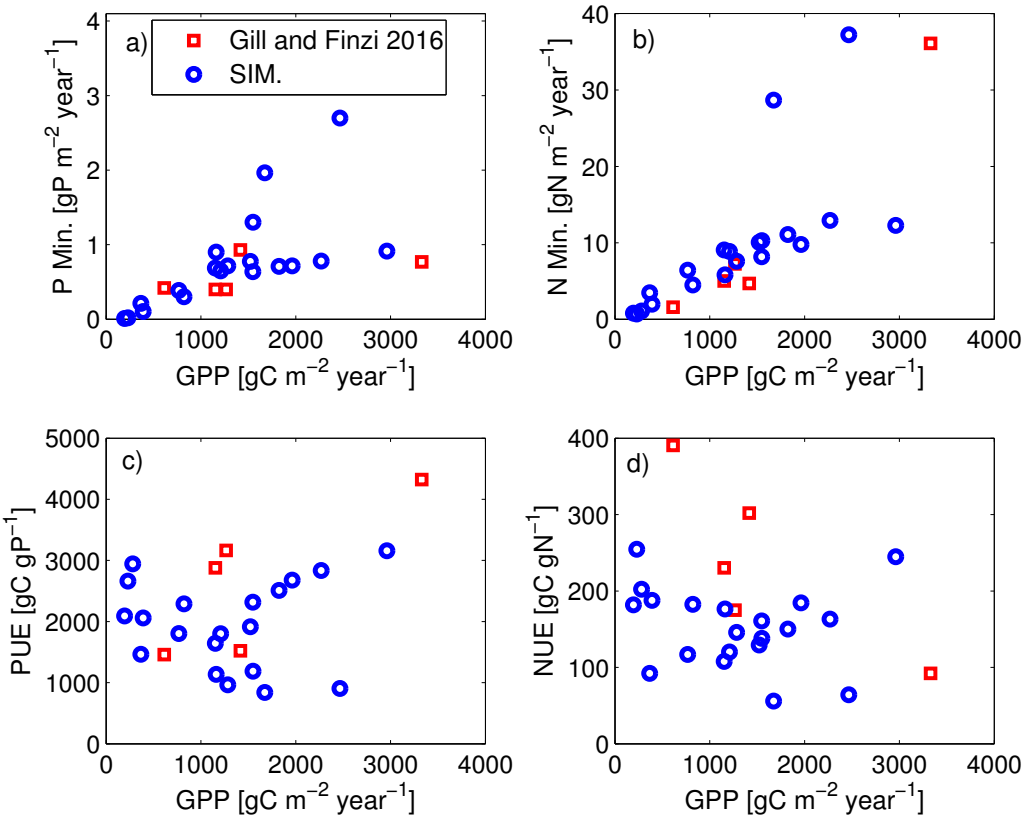

Figure 3. Scatter plots between Gross Primary Production (GPP) and (a) phosphorus mineralization (P Min.), (b) nitrogen mineralization (N Min.), (c) Phosphorus Use Efficiency (PUE), and (d) Nitrogen Use Efficiency (NUE). Circles are the time averaged simulated values for the 20 analyzed locations, the red squares are the values reported in Gill and Finzi (2016), which represent different biomes globally. Simulated NUE and PUE are computed as the ratio of GPP to the corresponding nutrient uptake rates.

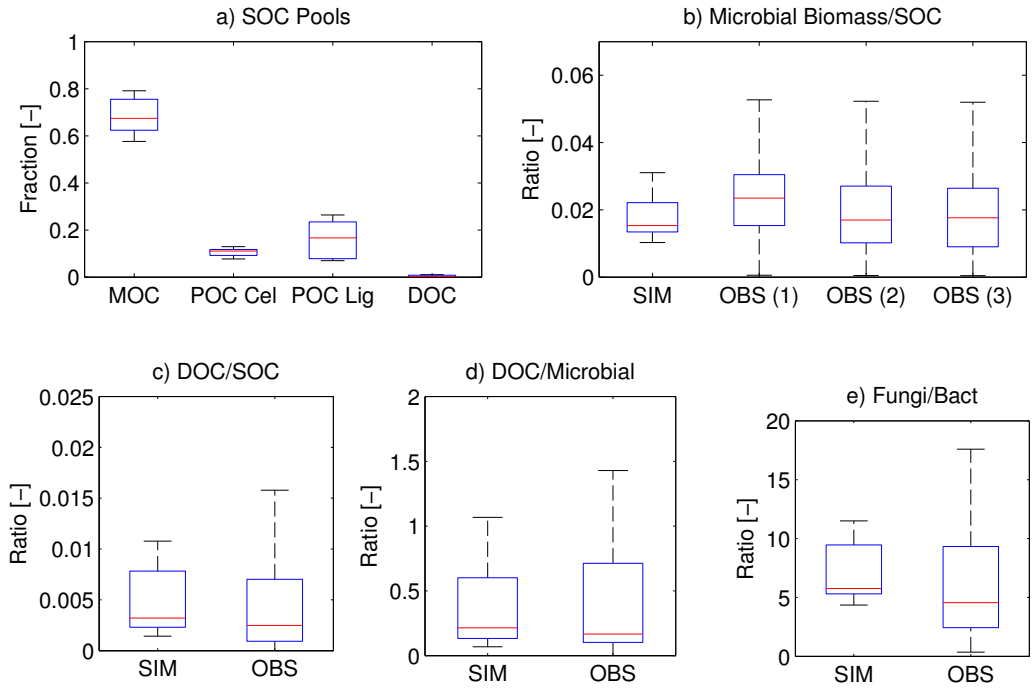

Figure 4. (a) Boxplot representation of the simulated variability in soil organic carbon (SOC) components for the 20 sites. The fractions of mineral-associated organic carbon (MOC), particulate organic carbon (POC) subdivided in POC-lignin (POC-Lig) and POC-cellulose/hemicellulose (POC-Cel) and dissolved organic carbon (DOC) are shown. (b) Boxplot representation of the simulated variability in the ratio between microbial biomass and SOC compared with observations reported by G. Wang et al. (2013) (OBS 1), Xu et al. (2013) (OBS 2), and Xu et al. (2017) (OBS 3). (c) Boxplot representation of the simulated variability of the ratio between DOC and SOC compared with observations reported by G. Wang et al. (2013). (d) Boxplot representation of the simulated variability of the ratio between DOC and microbial biomass compared with observations reported by G. Wang et al. (2013). (e) Boxplot representation of the simulated variability of the mass ratios between fungi and bacteria compared with observations reported by Waring et al. (2013). Boxplots include results for the 20 analyzed locations in terms of time averaged quantities. The central mark of each box is the median, the edges are the 25th and 75th percentiles, the whiskers extend to the most extreme data points that are not considered outliers.

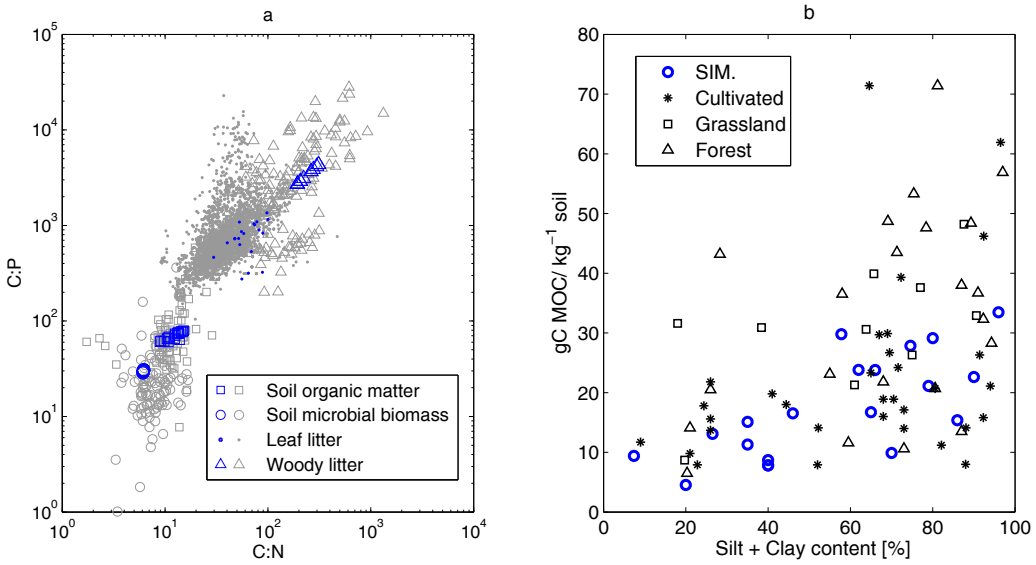

Figure 5. (a) Scatter plot between C:N mass ratio and C:P mass ratio in woody litter (triangles), leaf litter (points), soil organic matter (squares), and soil microbial biomass (circles) as simulated by T&C-BG for the 20 analyzed locations (blue) and from literature observations (gray). Data on litter and wood decomposition are from Manzoni et al. (2017) and data on soil and microbial biomass stoichiometry are from Cleveland and Liptzin (2007). (b) Scatter plot between the fraction of silt plus clay in the soil and the content of mineral associated organic carbon (MOC) for unit of soil volume as simulated for the 20 analyzed locations (blue) and reported from observations in Six et al. (2002) (black).

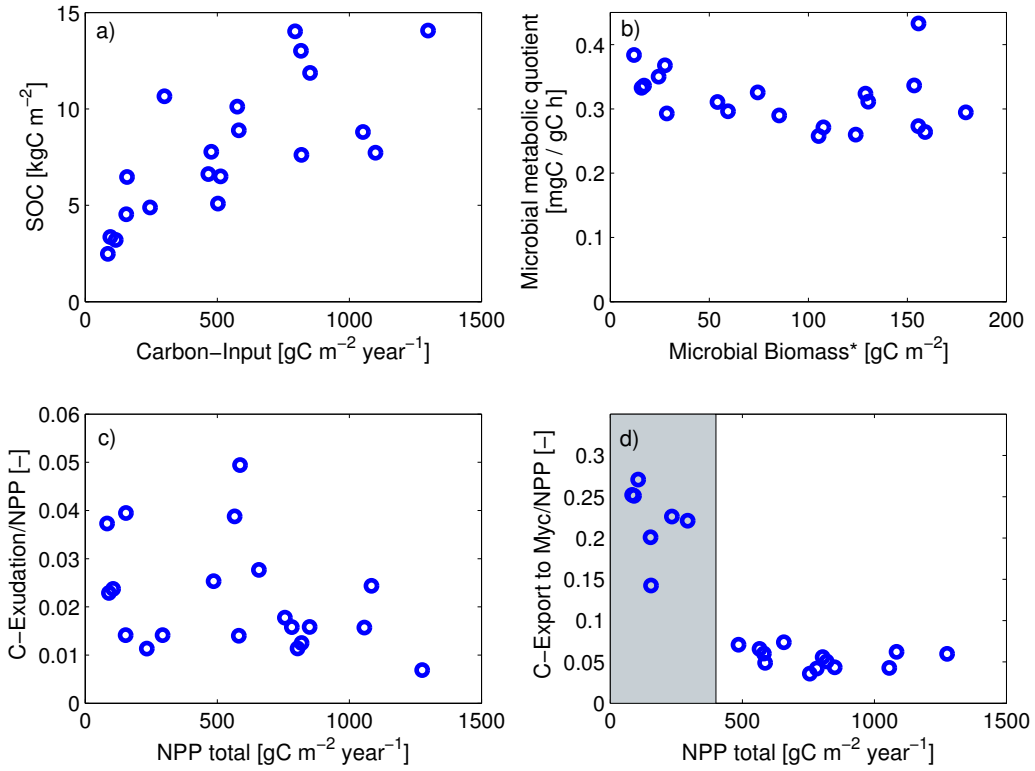

Figure 6. Scatter plots of simulated relations between (a) soil organic carbon (SOC) and total litter carbon input; (b) microbial metabolic quotient and microbial biomass*, i.e., microbial biomass excluding mycorrhiza fungi; (c) Net Primary Production (NPP) and the fraction of NPP allocated to C exudation; and (d) Net Primary Production (NPP) and the fraction of NPP exported to mycorrhiza fungi. The shaded area corresponds to values for which the confidence in model simulations is particularly low.

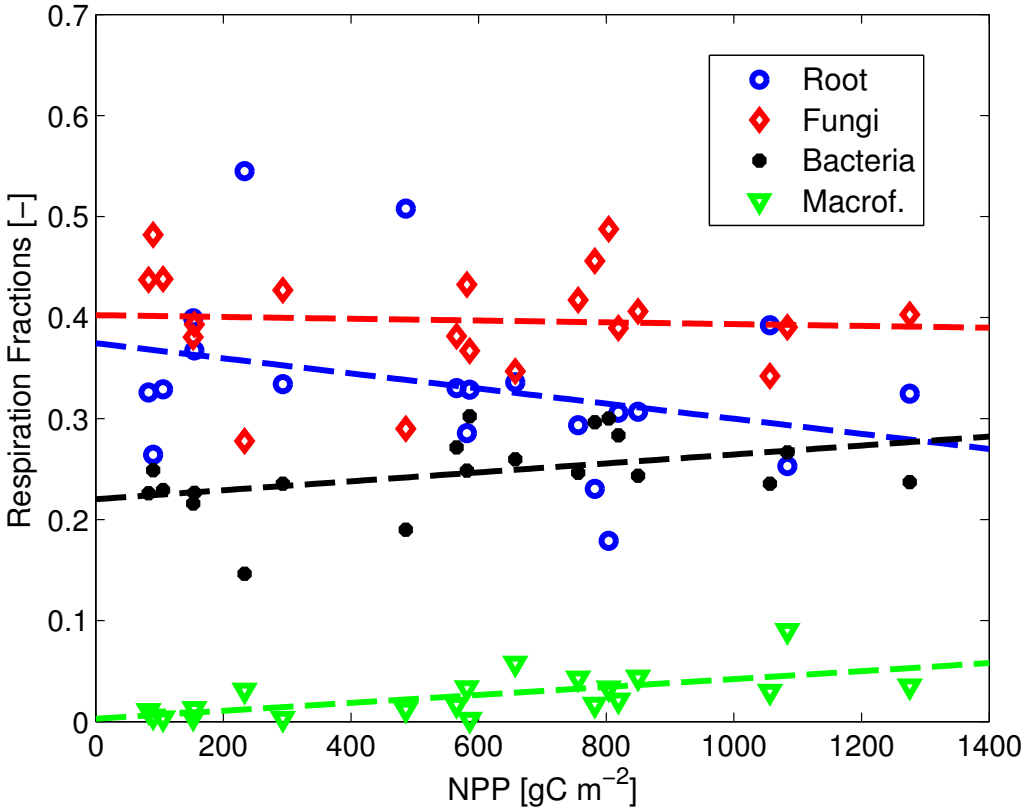

Figure 7. Partition of simulated soil respiration among the fractions contributed by fine-roots (circles), bacteria (dots), fungi (diamonds) and macrofauna (triangles) for each of the 20 analyzed locations regressed versus Net Primary Production (NPP). The dashed lines represent a linear ordinary least square fit to the points.

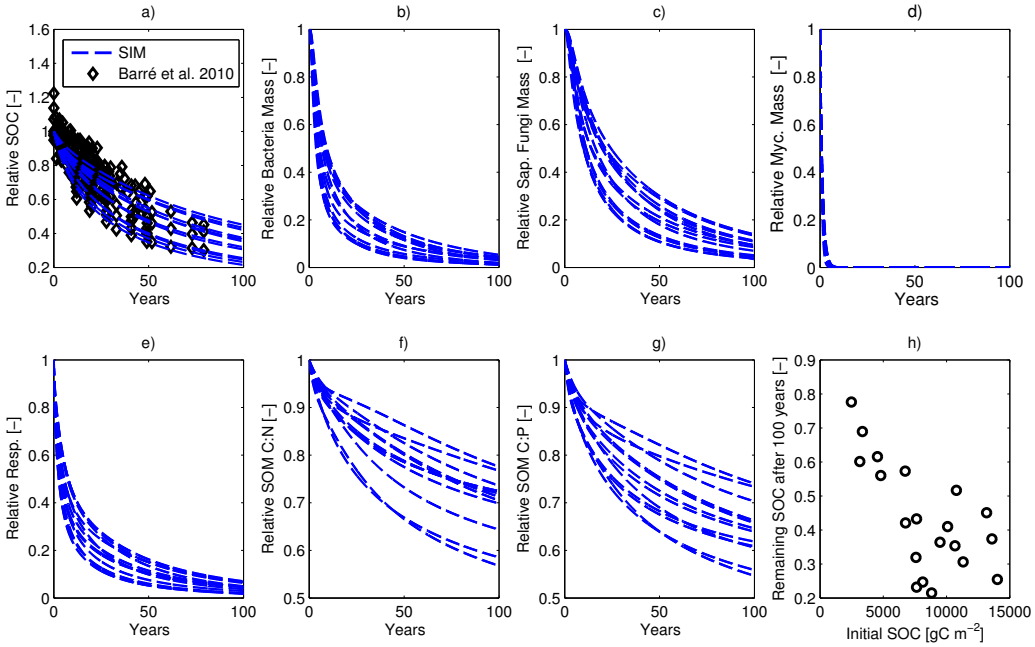

Figure 8. (a) Changes in soil organic carbon (SOC) through time normalized by the initial value of SOC in bare-fallow experiments. Dashed lines are results from the simulations for the 12 locations with more than 700 $mm\,year^{-1}$ of precipitation. Points correspond to results published for seven locations in Barré et al. (2010). Simulated changes through time normalized by the initial value during the bare-fallow experiments are also reported for (b) bacteria biomass; (c) saprotrophic fungi biomass; (d) mycorrhizal fungi biomass; (e) soil respiration; (f) C:N mass ratio of soil organic matter; (g) C:P mass ratio of soil organic matter. (h) Scatter plot between the initial SOC and the fraction of simulated SOC remaining after 100 years.

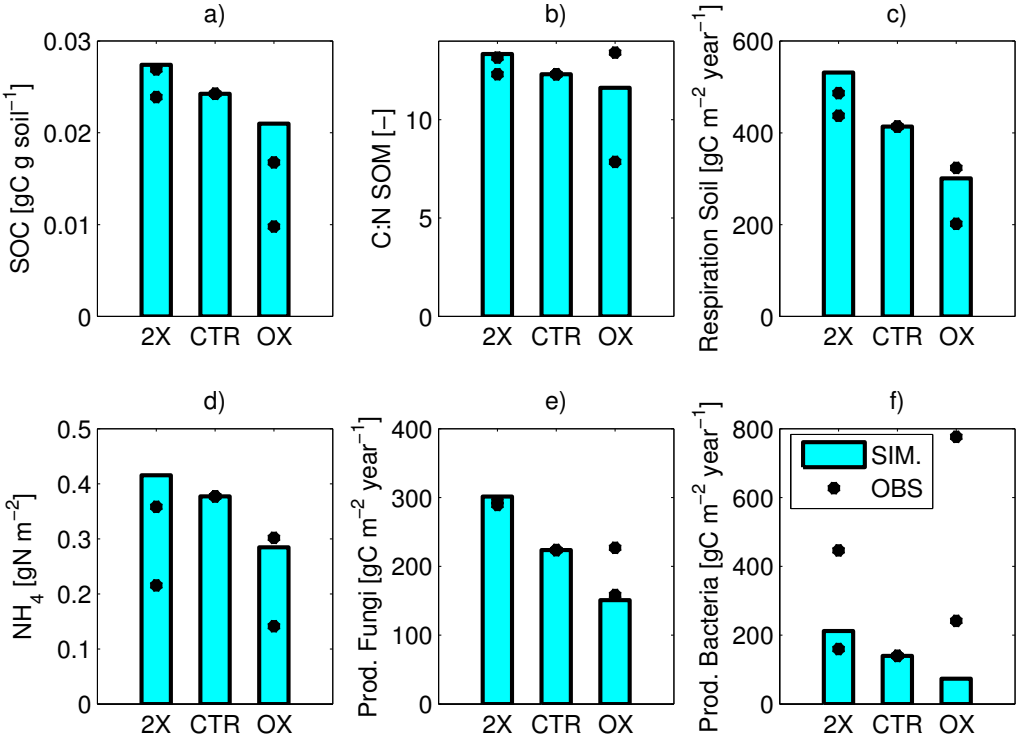

Figure 9. Simulated response to litter manipulation treatments in the Harvard forest location. The control scenario (CTR), corresponding to normal annual aboveground litter inputs, a double litter (2X, twice the litter inputs of the control plots), and no aboveground litter (0X, annual aboveground litter inputs excluded) scenarios are presented. Only the treatment effects (e.g., ratio between observed values in the different treatments) are used in the comparison. Simulated (bars) and observed (black points) are shown for: (a) soil organic carbon, (b) C:N mass ratio of soil organic matter, (c) soil respiration, (d) ammonium NH_4^+, (e) saprotrophic fungi productivity, (f) bacteria productivity. Observations for both mineral and organic soil layers are reported (two points for each treatment).

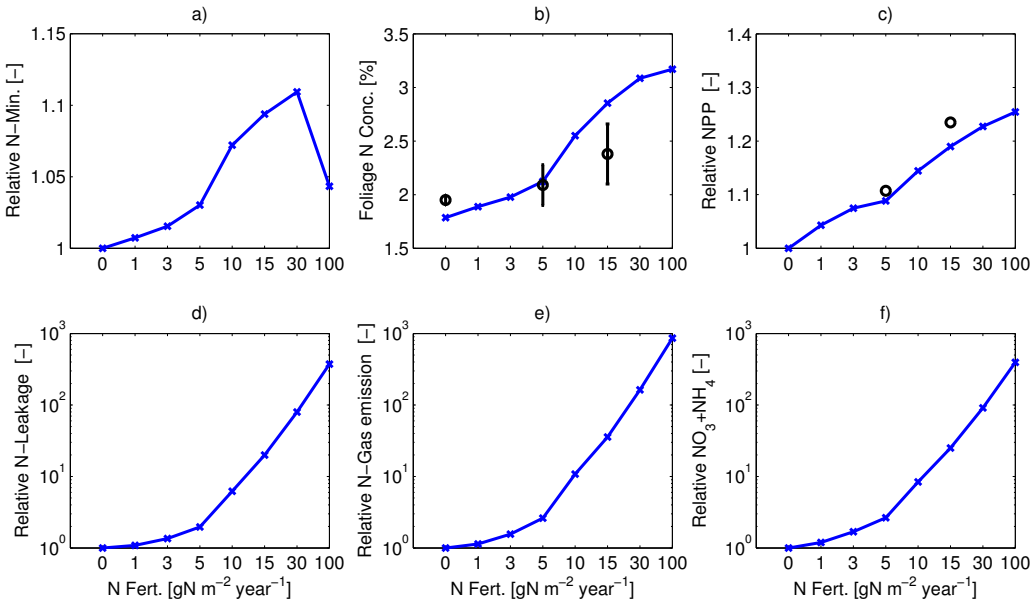

Figure 10. Simulated response to various levels of N-fertilization in the location of Little Prospect Hill (LPH). Changes are shown for: (a) net N-mineralization, (b) foliage nitrogen concentration, (c) Net Primary Production (NPP), (d) N leaching, (e) N - gas emissions, e.g., denitrification plus ammonia volatilization, (f) sum of ammonium NH_4^+ and nitrate NO_3^- nitrogen pools. Results are normalized with respect to the control scenario corresponding to lack of fertilization, except for foliage nitrogen concentration, where actual values are reported. Observations of changes in foliage N concetration and NPP in response to the 5 and 15 $gN\,m^{-2}\,year^{-1}$ treatments are also reported (black points) for comparison (Meyerholt & Zaehle, 2015).

Location	Lat.	Lon.	Biome	N. Yr.	P_r	T_a
Chamau (CH)	47.21	8.41	C3 Grassland	3.0	1156	9.7
Stubai (AT)	47.12	11.32	C3 Grassland	11.0	856	6.8
UMBS (MI,USA)	45.56	-84.71	Deciduous Forest	16.0	890	7.2
Manaus km34 (BR)	-2.61	-60.21	Tropical Forest	8.0	2737	25.8
Konza Praire (KS, USA)	39.10	-96.60	C3/C4 Grassland	31.7	826	12.8
Hyytiala (FI)	61.85	24.30	Evergreen Forest	16.0	707	4.2
Sevilleta grassland (NM, USA)	34.36	-106,70	C4 Grassland	4.0	239	13.4
Sevillata shrubland (NM, USA)	34.33	-106,74	Shrubs and C4 Grassland	4.0	226	14.1
ORNL FACE (TN, USA)	35.90	-84.33	Deciduous Forest	11.0	1221	14.8
Duke Forest (NC, USA)	35.96	-79.10	Evergreen Forest (Mostly)	12.0	1081	14.8
Harvard Forest (MA, USA)	42.54	-72.17	Deciduous Forest	19.2	1179	7.9
Morgan Monroe State Forest (IN, USA)	39.32	-86,41	Deciduous Forest	8.0	1068	12.3
Short Grass Steppe (CO, USA)	40.81	-104.75	C3/C4 Grassland	24.0	304	8.4
Willow Creek (WI, USA)	40.81	-90.08	Deciduous Forest	16.0	689	5.4
Vaira ranch (CA, USA)	38.41	-120.95	C3 Grassland	13.2	553	15.7
Kendall (AZ, USA)	31.74	-109.94	C3/C4 Grassland	9.6	280	17.4
Hainich (DE)	51.08	10,45	Deciduous Forest	8.0	806	8.3
Little Prospect Hill - LPH (MA, USA)	42.54	-72.54	Mixed Forest	8.0	1303	7.8
Jornada Basin (NM, USA)	32,51	-106.78	C3/C4 Grassland and Shrubs	21.0	249	18.1
TasFACE (AUS)	-42.70	147.26	C3/C4 Grassland	8.2	388	11.7

Table 1. Site characteristics for the 20 locations used in the analysis, latitude, longitude, length of the time series of meteorological drivers in years (N. Yr), biome description, mean precipitation (P_r) $[mm\,yr^{-1}]$ and mean air temperature (T_a) $[^{\circ}C]$ are reported.

Variable	**OBSERVED**	**SIMULATED**
$NEE\ UMBS\ [g\,C\,m^{-2}\,year^{-1}]$	-184	-122
$NEE\ Harvard\ [g\,C\,m^{-2}\,year^{-1}]$	-292	-189
UMBS	–	–
$AGWB$ 1998 $[g\,C\,m^{-2}]$	6470	5460
$AGWB$ 2006 $[g\,C\,m^{-2}]$	7745	5900
SOC $[g\,C\,m^{-2}]$	5500 - 8040	5034
N Min. $[g\,N\,m^{-2}\,year^{-1}]$	4.26	5.81
NO_3^- Leaching $[g\,N\,m^{-2}\,year^{-1}]$	0.001	0.011
N Gas-efflux $[g\,N\,m^{-2}\,year^{-1}]$	0.002	0.0054

Table 2. Observed and simulated quantities at UMBS and Harvard forests, where NEE is the Net Ecosystem Exchange, $AGWB$ is the aboveground standing wood biomass, SOC is the total soil organic carbon, and Min. stays for net-mineralization. Observations are derived from flux-tower measured NEE and published values for the other quantities (Gough et al., 2008; McFarlane et al., 2013; Nave et al., 2011, 2009).

Acknowledgments

This study was partially supported by the Swiss National Science Foundation (r4d - Ecosystems, n. 152019). SM was supported by the Swedish Research Councils Formas (grants 2015-468 and 2016-00998) and VR (grant 2016-04146). AP acknowledges funding from NERC (grant NE/S003495/1). The PIs of the FLUXNET community, the manipulation experiments, and the long-term research sites that acquired and shared data used to force and test the T&C model simulations are deeply acknowledged. All the data used in this article are from published articles and the corresponding source is properly cited and acknowledged. Detailed simulation results are available upon request to the corresponding author.

References

Aber, J. D., McDowell, W., Nadelhoffer, K., Magill, A., Berntson, G., Kamakea, M., ... Fernandez, I. (1998). Nitrogen saturation in temperate forest ecosystems - hypotheses revisited. *Bioscience*, *48*, 921-934.

Aber, J. D., Nadelhoffer, K. J., Steudler, P., & Melillo, J. M. (1989). Nitrogen saturation in northern forest ecosystems. *Bioscience*, *39*, 378-386.

Abramoff, R., Xu, X., Hartman, M., O'Brien, S., Feng, W., Davidson, E., ... Mayes, M. A. (2018). The Millennial model: in search of measurable pools and transformations for modeling soil carbon in the new century. *Biogeochemistry*, *137*, 51-71. (doi.org/10.1007/s10533-017-0409-7)

Ainsworth, E. A., & Long, S. P. (2005). What have we learned from 15 years of Free-Air CO_2 Enrichment (FACE)? A meta-analytic review of the responses of photosynthesis, canopy properties and plant production to rising CO_2. *New Phytologist*, *165*(2), 351-371.

Allison, S. D. (2005). Cheaters, diffusion, and nutrients constrain decomposition by microbial enzymes in spatially structured environments. *Ecol. Lett.*, *8*, 626-635.

Allison, S. D. (2012). A trait-based approach for modelling microbial litter decomposition. *Ecology Letters*, *15*, 1058-1070.

Allison, S. D. (2017). Microbial biomass: A paradigm shift in terrestrial biogeochemistry. In (chap. Building Predictive Models for Diverse Microbial Communities in Soil). UC Irvine. ([UCPMS ID)

Allison, S. D., Wallenstein, M. D., & Bradford, M. A. (2010). Soil-carbon response to warming dependent on microbial physiology. *Nature Geosciences*, *3*, 336-340.

Ananyeva, N. D., Castaldi, S., Stolnikova, E. V., Kudeyarov, V. N., & Valentini, R. (2015). Fungi-to-bacteria ratio in soils of european russia. *Archives of Agronomy and Soil Science*, *61*(4), 427-446.

Anderson, T.-H., & Domsch, K. H. (1989). Ratios of microbial biomass carbon to total organic carbon in arable soil. *Soil Biology & Biogeochemistry*, *21*(4), 471-479.

Aoyama, M., Angers, D. A., & N'Dayegamiye, A. (1999). Particulate and mineral-associated organic matter in waterstable aggregates as affected by mineral fertilizer and manure applications. *Canadian Journal of Soil Science*, *79*, 295-302.

Averill, C., Waring, B. G., & Hawkes, C. V. (2016). Historical precipitation predictably alters the shape and magnitude of microbial functional response to soil moisture. *Global Change Biology*, *22*, 1957-1964.

Bååth, E., Nilsson, L. O., Göransson, H., & Wallander, H. (2004). Can the extent of degradation of soil fungal mycelium during soil incubation be used to estimate ectomycorrhizal biomass in soil? *Soil Biology and Biochemistry*, *36*, 2105-2109.

Barré, P., Eglin, T., Christensen, B. T., Ciais, P., Houot, S., Kätterer, T., ... Chenu, C. (2010). Quantifying and isolating stable soil organic carbon using long-term bare fallow experiments. *Biogeosciences*, *7*, 3839-3850.

Baskaran, P., Hyvönen, R., Berglund, S. L., Clemmensen, K. E., Ågren, G. I., Lindahl, B. D., & Manzoni, S. (2017). Modelling the influence of ectomycorrhizal decomposition on plant nutrition and soil carbon sequestration in boreal forest ecosystems. *New Phytologist*, *213*(3), 1452-1465.

Batterman, S. A., Hedin, L. O., van Breugel, M., Ransijn, J., Craven, D. J., & Hall, J. S. (2013). Key role of symbiotic dinitrogen fixation in tropical forest secondary succession. *Nature*, *502*, 224-227.

Bonan, G. B., Lawrence, P. J., Oleson, K. W., Levis, S., Jung, M., Reichstein, M., ... Swenson, S. C. (2011). Improving canopy processes in the Community Land Model version 4 (CLM4) using global flux fields empirically inferred from FLUXNET data. *Journal of Geophysical Research*, *116*(G02014). (doi:10.1029/2010JG001593)

Bonan, G. B., Levis, S., Kergoat, L., & Oleson, K. W. (2002). Landscapes as patches of plant functional types: An integrating concept for climate and ecosystem models. *Global Biogeochemical Cycles*, *16*(2,1021). (doi:10.1029/2000GB001360)

Bond-Lamberty, B., Bailey, V. L., Chen, M., Gough, C. M., & Vargas, R. (2018). Globally rising soil heterotrophic respiration over recent decades. *Nature*, *560*, 80-83.

Bowden, R. D., Nadelhoffer, K. J., Boone, R. D., Meillo, J. M., & Garrison., J. B. (1993). Contributions of aboveground litter, belowground litter, and root respiration to total soil respiration in a temperate mixed hardwood forest. *Canadian Journal of Forest Research*, *23*, 1402-1407.

Bradford, M. A., & Fierer, N. (2012). Soil ecology and ecosystem services. In D. H. Wall (Ed.), (p. 189-200). Oxford, UK: Oxford University Press.

Brundrett, M. C. (2009). Mycorrhizal associations and other means of nutrition of vascular plants: understanding the global diversity of host plants by resolving conflicting information and developing reliable means of diagnosis. *Plant and Soil*, *320*, 37-77. (doi:10.1007/s11104-008-9877-9)

Brzostek, E. R., Fisher, J. B., & Phillips, R. P. (2014). Modeling the carbon cost of plant nitrogen acquisition: Mycorrhizal trade-offs and multipath resistance uptake improve predictions of retranslocation. *J. Geophys. Res. Biogeosci*, *119*, 1684-1697. (doi:10.1002/2014JG002660)

Brzostek, E. R., Greco, A., Drake, J. E., & Finzi, A. C. (2013). Root carbon inputs to the rhizosphere stimulate extracellular enzyme activity and increase nitrogen availability in temperate forest soils. *Biogeochemistry*, *115*(1-3), 65-76.

Buendia, C., Kleidon, A., & Porporato, A. (2010). The role of tectonic uplift, climate, and vegetation in the long-term terrestrial phosphorous cycle. *Biogeosciences*, *7*, 2025-2038.

Cambardella, C. A., & Elliott, E. T. (1992). Particulate soil organic-matter changes across a grassland cultivation sequence. *Soil Sci. Soc. Am. J.*, *56*, 777-783.

Campbell, E. E., Parton, W. J., Soong, J. L., Paustian, K., Hobbs, N. T., & Cotrufo, M. F. (2016). Using litter chemistry controls on microbial processes to partition litter carbon fluxes with the litter decomposition and leaching (LIDEL) model. *Soil Biology and Biochemistry*, *100*, 160-174.

Carvalhais, N., Forkel, M., Khomik, M., Bellarby, J., Jung, M., Migliavacca, M., ... Reichstein, M. (2014). Global covariation of carbon turnover times with climate in terrestrial ecosystems. *Nature*, *514*, 213-217.

Chapin III, F. S., Schulze, E.-D., & Mooney, H. A. (1990). The ecology and economics of storage in plants. *Annual Review of Ecology and Systematics*, *21*, 423-447.

Chertov, O., Shaw, C., Shashkov, M., Komarov, A., Bykhovets, S., Shanin, V., ...

Zubkova, E. (2017). Romulhum model of soil organic matter formation coupled with soilbiota activity. III. Parameterisation of earthworm activity. *Ecological Modelling*, *345*, 140-149.

Clark, D. B., Mercado, L. M., Sitch, S., Jones, C. D., Gedney, N., Best, M. J., ... Cox, P. M. (2011). The Joint UK Land Environment Simulator (jules), model description - Part 2: Carbon fluxes and vegetation dynamics. *Geosci. Model Dev.*, *4*(3), 701-722.

Clemmensen, K., Bahr, A., Ovaskainen, O., Dahlberg, A., Ekblad, A., Wallander, H., ... Lindahl, B. (2013). Roots and associated fungi drive long-term carbon sequestration in boreal forest. *Science*, *339*, 1615-1618.

Cleveland, C. C., Houlton, B. Z., Smith, W. K., Marklein, A. R., Reed, S. C., Parton, W., ... Running, S. W. (2013). Patterns of new versus recycled primary production in the terrestrial biosphere. *Proc. Natl Acad. Sci. USA*, *110*, 12733-12737.

Cleveland, C. C., & Liptzin, D. (2007). C:N:P stoichiometry in soil: is there a redfield ratio for the microbial biomass? *Biogeochemistry*, *85*, 235-252.

Cleveland, C. C., Townsend, A. R., Schimel, D. S., Fisher, H., Howarth, R. W., Hedin, L. O., ... Wasson, M. F. (1999). Global patterns of terrestrial biological nitrogen (N_2) fixation in natural ecosystems. *Glob. Biogeochem. Cycles*, *13*, 623-645.

Compton, J. E., Watrud, L. S., Porteous, L. A., & DeGrood, S. (2004). Response of soil microbial biomass and community composition to chronic nitrogen additions at harvard forest. *Forest Ecology and Management*, *196*, 143-158.

Conant, R. T., Ryan, M. G., Ågren, G. I., Birge, H. E., Davidson, E. A., Eliasson, P. E., ... Bradford, M. A. (2011). Temperature and soil organic matter decomposition rates-synthesis of current knowledge and a way forward. *Global Change Biology*, *17*, 3392-3404.

Crowther, T. W., Todd-Brown, K. E. O., Rowe, C. W., Wieder, W. R., Carey, J. C., Machmuller, M. B., ... Bradford, M. A. (2016). Quantifying global soil carbon losses in response to warming. *Nature*, *540*, 104-108.

Curry, J. P. (1998). Earthworm ecology. In A. Edwards (Ed.), (p. 37-64). St. Lucie Press, Boca Raton FL.

Curry, J. P., & Schmidt, O. (2007). The feeding ecology of earthworms - a review. *Pedobiologia*, *50*, 463-477.

Curtis, P. S., Hanson, P. J., Bolstad, P., Barford, C., Randolph, J. C., Schmid, H. P., & Wilson, K. B. (2002). Biometric and eddy-covariance based estimates of annual carbon storage in five eastern North American deciduous forests. *Agricultural and Forest Meteorology*, *113*, 3-19.

Curtis, P. S., Vogel, C. S., Gough, C. M., Schmid, H. P., Su, H. B., & Bovard, B. D. (2005). Respiratory carbon losses and the carbon-use efficiency of a northern hardwood forest, 1999-2003. *New Phytologist*, *167*(2), 437-455.

Daly, E., & Porporato, A. (2005). A review of soil moisture dynamics: from rainfall infiltration to ecosystem response. *Environmental Engineering Science*, *22*(1), 9-24.

Dentener, F. J. (2006). *Global maps of atmospheric nitrogen deposition, 1860, 1993, and 2050.* Available on-line [http://daac.ornl.gov/] from Oak Ridge National Laboratory Distributed Active Archive Center, Oak Ridge, Tennessee, U.S.A. doi:10.3334/ORNLDAAC/830. (Data set)

Dickinson, R. E., Berry, J. A., Bonan, G. B., Collatz, G. J., Field, C. B., Fung, I. Y., ... Shaikh, M. (2002). Nitrogen controls on climate model evapotranspiration. *Journal of Climate*, *15*, 278-294.

Ebrahimi, A., & Or, D. (2016). Microbial community dynamics in soil aggregates shape biogeochemical gas fluxes from soil profiles - upscaling an aggregate biophysical model. *Global Change Biol.*, *22*(9), 3141-3156. (doi:10.1111/gcb.13345)

Ebrahimi, A., & Or, D. (2017). Mechanistic modeling of microbial interactions at pore to profile scale resolve methane emission dynamics from permafrost soil. *J. Geophys. Res. Biogeosci.*, *122*. (doi:10.1002/2016JG003674)

Ekblad, A., Wallander, H., Godbold, D. L., Cruz, C., Johnson, D., Baldrian, P., ... Plassard, C. (2013). The production and turnover of extramatrical mycelium of ectomycorrhizal fungi in forest soils: role in carbon cycling. *Plant and Soil*, *366*, 1-27.

Fahey, T. J., Yavitt, J. B., Sherman, R. E., Maerz, J. C., Groffman, P. M., Fisk, M. C., & Bohlen, P. J. (2013). Earthworms, litter and soil carbon in a northern hardwood forest. *Biogeochemistry*, *114*, 269-280. (doi:10.1007/s10533-012-9808-y)

Farquhar, G. D., Caemmerer, S. V., & Berry, J. A. (1980). A biochemical model of photosynthetic CO_2 assimilation in leaves of C3 species. *Planta*, *149*, 78-90.

Fatichi, S., & Ivanov, V. Y. (2014). Interannual variability of evapotranspiration and vegetation productivity. *Water Resources Research*, *50*, 3275-3294. (doi:10.1002/2013WR015044)

Fatichi, S., Ivanov, V. Y., & Caporali, E. (2011). Simulation of future climate scenarios with a weather generator. *Advances in Water Resources*, *34*, 448-467. (doi:10.1016/j.advwatres.2010.12.013)

Fatichi, S., Ivanov, V. Y., & Caporali, E. (2012). A mechanistic ecohydrological model to investigate complex interactions in cold and warm water-controlled environments. 1 Theoretical framework and plot-scale analysis. *Journal of Advances in Modeling Earth Systems*, *4*(M05002).

Fatichi, S., Katul, G. G., Ivanov, V. Y., Pappas, C., Paschalis, A., Consolo, A., ... Burlando, P. (2015). Abiotic and biotic controls of soil moisture spatiotemporal variability and the occurrence of hysteresis. *Water Resources Research*, *51*(5), 3505-3524. (doi:10.1002/2014WR016102)

Fatichi, S., & Leuzinger, S. (2013). Reconciling observations with modeling: the fate of water and carbon allocation in a mature deciduous forest exposed to elevated CO_2. *Agricultural and Forest Meteorology*, *174-175*, 144-157. (doi:10.1016/j.agrformet.2013.02.005)

Fatichi, S., Leuzinger, S., Paschalis, A., Langley, J. A., Barraclough, A. D., & Hovenden, M. (2016). Partitioning direct and indirect effects reveals the response of water limited ecosystems to elevated CO_2. *Proceedings of the National Academy of Sciences USA*, *113*(45), 12757-12762. (doi: 10.1073/pnas.1605036113)

Fatichi, S., & Pappas, C. (2017). Constrained variability of modeled T:ET ratio across biomes. *Geophysical Research Letters*, *44*, –. (doi:10.1002/2017GL074041)

Fatichi, S., Zeeman, M. J., Fuhrer, J., & Burlando, P. (2014). Ecohydrological effects of management on subalpine grasslands: from local to catchment scale. *Water Resources Research*, *50*. (doi:10.1002/2013WR014535)

Fenn, K. M., Malhi, Y., & Morecroft, M. D. (2010). Soil CO_2 efflux in a temperate deciduous forest: Environmental drivers and component contributions. *Soil Biology & Biochemistry*, *42*, 1685-1693.

Fierer, N., & Jackson, R. B. (2006). The diversity and biogeography of soil bacterial communities. *Proceedings of the National Academy of Sciences of the United States of America*, *103*(3), 626-631.

Fierer, N., Strickland, M. S., Liptzin, D., Bradford, M. A., & Cleveland, C. C. (2009). Global patterns in belowground communities. *Ecology Letters*, *12*, 1238-1249. (doi: 10.1111/j.1461-0248.2009.01360.x)

Finlay, R. D. (2008). Ecological aspects of mycorrhizal symbiosis: with special emphasis on the functional diversity of interactions involving the extraradical mycelium. *Journal of Experimental Botany*, *59*(5), 1115-1126.

Fisher, J. B., Sitch, S., Malhi, Y., Fisher, R. A., Huntingford, C., & Tan, S.-Y.

(2010). Carbon cost of plant nitrogen acquisition: a mechanistic, globally applicable model of plant nitrogen uptake, retranslocation, and fixation. *Global Biogeochemical Cycles*, *24*, GB1014.

Foley, J. (1995). An equilibrium model of the terrestrial carbon budget. *Tellus B*, *47*, 310-319.

Freschet, G. T., Aerts, R., & Cornelissen, J. H. C. (2012). A plant economics spectrum of litter decomposability. *Functional Ecology*, *26*, 56-65.

Frey, S. D., Lee, J., Melillo, J. M., & Six, J. (2013). The temperature response of soil microbial efficiency and its feedback to climate. *Nature Clim. Change*, *3*, 395-398.

Frey, S. D., Ollinger, S., Nadelhoffer, K., Bowden, R., Brzostek, E., Burton, A., ... Wickings, K. (2014). Chronic nitrogen additions suppress decomposition and sequester soil carbon in temperate forests. *Biogeochemistry*, *121*, 305-316.

Friedlingstein, P., Meinshausen, M., Arora, V. K., Jones, C. D., Anav, A., Liddicoat, S. K., & Knutti, R. (2014). Uncertainties in CMIP5 climate projections due to carbon cycle feedbacks. *Journal of Climate*, *27*, 511-526.

Friend, A. D., & Kiang, N. Y. (2005). Land-surface model development for the GISS GCM: Effects of improved canopy physiology on simulated climate. *Journal of Climate*, *18*, 2833-2902.

Friend, A. D., Stevens, A. K., Knox, R. G., & Cannell, M. G. R. (1997). A process-based, terrestrial biosphere model of ecosystem dynamics (Hybrid v3.0). *Ecological Modelling*, *95*, 249-287.

Galloway, J. N., Dentener, F. J., Capone, D. G., Boyer, E. W., Howarth, R. W., Seitzinger, S. P., ... Vörösmarty., C. (2004). Nitrogen cycles:ast, present and future. *Biogeochemistry*, *70*, 153-226.

Georgiou, K., Abramoff, R. Z., Harte, J., Riley, W. J., & Torn, M. S. (2017). Microbial community-level regulation explains soil carbon responses to long-term litter manipulations. *Nat Commun*, *8*, 1223.

Gill, A. L., & Finzi, A. C. (2016). Belowground carbon flux links biogeochemical cycles and resource-use efficiency at the global scale. *Ecology Letters*, *19*, 1419-1428.

Goll, D. S., Brovkin, V., Parida, B. R., Reick, C. H., Kattge, J., Reich, P. B., ... Niinemets, U. (2012). Nutrient limitation reduces land carbon uptake in simulations with a model of combined carbon, nitrogen and phosphorus cycling. *Biogeosciences*, *9*, 3547-3569. (doi:10.5194/bg-9-3547-2012)

Goll, D. S., Winkler, A. J., Raddatz, T., Dong, N., Prentice, I. C., Ciais, P., & Brovkin, V. (2017). Carbon-nitrogen interactions in idealized simulations with JSBACH (version 3.10). *Geoscientific Model Development*, *10*, 2009-2030.

Gough, C. M., Vogel, C. S., Kazanski, C., Nagel, L., Flower, C. E., & Curtis, P. S. (2007). Coarse woody debris and the carbon balance of a north temperate forest. *Forest Ecology Management*, *244*(1-3), 60-67.

Gough, C. M., Vogel, C. S., Schmid, H. P., & Curtis, P. S. (2008). Controls on annual forest carbon storage: Lessons from the past and predictions for the future. *Bioscience*, *58*, 609-622.

Hanson, C. A., Allison, S. D., Bradford, M. A., Wallenstein, M. D., & Treseder, K. K. (2008). Fungal taxa target different carbon sources in forest soil. *Ecosystems*, *11*(7), 1157-1167.

Hashimoto, S., Carvalhais, N., Ito, A., Migliavacca, M., Nishina, K., & Reichstein, M. (2015). Global spatiotemporal distribution of soil respiration modeled using a global database. *Biogeosciences*, *12*, 4121-4132. (doi:10.5194/bg-12-4121-2015)

Hassink, J., & Whitmore, A. P. (1997). A model of the physical protection of organic matter in soils. *Soil Sci. Soc. Am. J.*, *61*, 131-139.

Haynes, R. J. (1990). Active ion uptake and maintenance of cation-anion balance: A critical examination of their role in regulating rhizosphere pH. *Plant and Soil*,

126(2), 247-264.

Hinsinger, P., Brauman, A., Devau, N., Gérard, F., Jourdan, C., Laclau, J.-P., ... Plassard, C. (2011). Acquisition of phosphorus and other poorly mobile nutrients by roots. Where do plant nutrition models fail? *Plant Soil*, *348*, 29-61. (doi:10.1007/s11104-011-0903-y)

Hobbie, E. A. (2006). Carbon allocation to ectomycorrhizal fungi correlates with belowground allocation in culture studies. *Ecology*, *87*(3), 563-569.

Högberg, M. N., & Högberg, P. (2002). Extramatrical ectomycorrhizal mycelium contributes one-third of microbial biomass and produces, together with associated roots, half the dissolved organic carbon in a forest soil. *New Phytol.*, *154*(3), 791-795.

Högberg, P., Nordgren, A., Buchmann, N., Taylor, A. F. S., Ekblad, A., Högberg, M. N., ... Read, D. J. (2001). Large-scale forest girdling shows that current photosynthesis drives soil respiration. *Nature*, *411*, 789-792.

Holland, E. A., Post, W. M., Matthews, E. G., Sulzman, J. M., Staufer, R., & Krankina, O. N. (2014). *A global database of litterfall mass and litter pool carbon and nutrients* (Tech. Rep.). ORNL DAAC, Oak Ridge, Tennessee, USA. (doi.org/10.3334/ORNLDAAC/1244)

Houlton, B. Z., Morford, S. L., & Dahlgren, R. A. (2018). Convergent evidence for widespread rock nitrogen sources in Earth's surface environment. *Science*, *360*(6384), 58-62.

Jackson, R. B., Mooney, H. A., & Schulze, E. D. (1997). A global budget for fine root biomass, surface area, and nutrient contents. *Proc. Natl. Acad. Sci. USA*, *94*, 7362-7366.

Joergensen, R. G., & Wichern, F. (2008). Quantitative assessment of the fungal contribution to microbial tissue in soil. *Soil Biology & Biochemistry*, *40*, 2977-2991.

Johnson, N. C., Angelard, C., Sanders, I. R., & Kiers, E. T. (2013). Predicting community and ecosystem outcomes of mycorrhizal responses to global change. *Ecology Letters*, *16*, 140-153. (doi: 10.1111/ele.12085)

Jungk, A. O. (2002). Plant roots: the hidden half. In Y. Waisel, A. Eshel, & U. Kafkafi (Eds.), (p. 587-616). Marcel Dekker Inc., New York.

Keeling, R. F., Piper, S. C., Bollenbacher, A. F., & Walker, J. S. (2009). *Atmospheric co_2 records from sites in the sio air sampling network, in trends: A compendium of data on global change* (Tech. Rep.). Carbon Dioxide Information Analysis Center, Oak Ridge Natl. Lab., U.S. Dep. of Energy, Oak Ridge, Tenn. (doi:10.3334/CDIAC/atg.035)

Keenan, T. F., Hollinger, D. Y., Bohrer, G., Dragoni, D., Munger, J. W., Schmid, H. P., & Richardson, A. D. (2013). Increase in forest water-use efficiency as atmospheric carbon dioxide concentrations rise. *Nature*, *499*(7458), 324-327. (doi:10.1038/nature12291)

Kirschbaum, M. U. F., & Paul, K. I. (2002). Modelling C and N dynamics in forest soils with a modified version of the CENTURY model. *Soil Biology & Biochemistry*, *34*, 341-354.

Kögel-Knabner, I. (2002). The macromolecular organic composition of plant and microbial residues as inputs to soil organic matter. *Soil Biology and Biochemistry*, *34*, 139-162.

Koide, R. T., Sharda, J. N., Herr, J. R., & Malcolm, G. M. (2008). Ectomycorrhizal fungi and the biotrophy-saprotrophy continuum. *New Phytologist*, *178*, 230-233.

Koven, C. D., Riley, W. J., Subin, Z. M., Tang, J. Y., Torn, M. S., Collins, W. D., ... Swenson, S. C. (2013). The effect of vertically resolved soil biogeochemistry and alternate soil C and N models on C dynamics of CLM4. *Biogeosciences*, *10*, 7109-7131.

Krinner, G., Viovy, N., de Noblet-Ducoudre, N., Ogee, J., Polcher, J., Friedlingstein,

P., ... Prentice, I. C. (2005). A dynamic global vegetation model for studies of the coupled atmosphere-biosphere system. *Global Biogeochemical Cycles*, *19*(GB1015). (doi:10.1029/2003GB002199)

Lawrence, C. R., Neff, J. C., & Schimel, J. P. (2009). Does adding microbial mechanisms of decomposition improve soil organic matter models? A comparison of four models using data from a pulsed rewetting experiment. *Soil Biology and Biochemistry*, *41*, 1923-1934.

Le Bauer, D. S., & Treseder, K. K. (2008). Nitrogen limitation of net primary productivity in terrestrial ecosystems is globally distributed. *Ecology*, *89*, 371-379.

Li, J., Wang, G., Allison, S. D., Mayes, M. A., & Luo, Y. (2014). Soil carbon sensitivity to temperature and carbon use efficiency compared across microbial-ecosystem models of varying complexity. *Biogeochemistry*, *119*, 67-84. (doi:10.1007/s10533-013-9948-8)

Lindahl, B. D., & Tunlid, A. (2015). Ectomycorrhizal fungi - potential organic matter decomposers, yet not saprotrophs. *New Phytologist*, *205*(4), 1443-1447. (doi:10.1111/nph.13201)

Long, T., & Or, D. (2005). Aquatic habitats and diffusion constraints affecting microbial coexistence in unsaturated porous media. *Water Resources Research*, *41*, 1-10.

Lubbers, I. M., van Groenigen, K. J., Fonte, S. J., Six, J., Brussaard, L., & van Groenigen, J. W. (2013). Greenhouse-gas emissions from soils increased by earthworms. *Nature Climate Change*, *3*, 187-194. (doi:10.1038/nclimate1692)

Magill, A. H., Aber, J. D., Currie, W. S., Nadelhoffer, K. J., Martin, M. E., McDowell, W. H., ... Steudler, P. (2004). Ecosystem response to 15 years of chronic nitrogen additions at the Harvard Forest LTER, Massachusetts, USA. *Forest Ecology and Management*, *196*, 7-28.

Mahowald, N., Jickells, T. D., Baker, A. R., Artaxo, P., Benitez-Nelson, C. R., Bergametti, G., ... Tsukud, S. (2008). Global distribution of atmospheric phosphorus sources, concentrations and deposition rates, and anthropogenic impacts. *Global Biogeochem. Cycles*, *22*, GB4026. (doi:10.1029/2008GB003240)

Manoli, G., Ivanov, V. Y., & Fatichi, S. (2018). Dry season greening and water stress in amazonia: the role of modeling leaf phenology. *Journal of Geophysical Research-Biogeosciences*, *123*, 1909-1926. (doi:10.1029/2017JG004282)

Manzoni, S. (2017). Flexible carbon-use efficiency across litter types and during decomposition partly compensates nutrient imbalances-results from analytical stoichiometric models. *Front Microbiol.*, *8*(661). (doi:10.3389/fmicb.2017.00661)

Manzoni, S., Jackson, R. B., Trofymow, J. A., & Porporato, A. (2008). The global stoichiometry of litter nitrogen mineralization. *Science*, *321*(684-686), 89-106.

Manzoni, S., Moyano, F., Kätterer, T., & Schimel, J. (2016). Modeling coupled enzymatic and solute transport controls on decomposition in drying soils. *Soil Biology & Biochemistry*, *95*, 275-287.

Manzoni, S., & Porporato, A. (2009). Soil carbon and nitrogen mineralization: Theory and models across scales. *Soil Biology & Biochemistry*, *41*, 1355-1379. (doi:10.1016/j.soilbio.2009.02.031)

Manzoni, S., Schimel, J. P., & Porporato, A. (2012). Responses of soil microbial communities to water stress: results from a meta-analysis. *Ecology*, *93*, 930-938.

Manzoni, S., Trofymow, J. A., Jackson, R. B., & Porporato, A. (2010). Stoichiometric controls on carbon, nitrogen, and phosphorus dynamics in decomposing litter. *Ecological Monographs*, *80*(1), 89-106.

Manzoni, S., Čapek, P., Mooshammer, M., Lindahl, B. D., Richter, A., & Šantručková, H. (2017). Optimal metabolic regulation along re-

source stoichiometry gradients. *Ecology Letters*, *20*, 1182-1191. (doi.org/10.1111/ele.12815)

Manzoni, S., Vico, G., Katul, G., Palmroth, S., & Porporato, A. (2014). Optimal plant water-use strategies under stochastic rainfall. *Water Resources Research*, *50*, 5379-5394. (doi:10.1002/2014WR015375)

Marschner, H., & Dell, B. (1994). Nutrient uptake in mycorrhizai symbiosis. *Plant and Soil*, *159*, 89-102.

Mastrotheodoros, T., Pappas, C., Molnar, P., Burlando, P., Keenan, T., Gentine, P., ... Fatichi, S. (2017). Linking plant functional trait plasticity and the large increase in forest water use efficiency. *Journal of Geophysical Research-Biogeosciences*, *122*(9), 2393-2408. (doi: 10.1002/2017JG003890)

McCarthy, H. R., Oren, R., Johnsen, K. H., Gallet-Budynek, A., Pritchard, S. G., Cook, C. W., ... Finzi, A. C. (2010). Re-assessment of plant carbon dynamics at the duke free-air CO_2 enrichment site: interactions of atmospheric [CO_2] with nitrogen and water availability over stand development. *New Phytologist*, *185*, 514-528. (doi: 10.1111/j.1469-8137.2009.03078.x)

McFarlane, K. J., Torn, M. S., Hanson, P. J., Porras, R. C., Swanston, C. W., Callaham Jr., M. A., & Guilderson, T. P. (2013). Comparison of soil organic matter dynamics at five temperate deciduous forests with physical fractionation and radiocarbon measurements. *Biogeochemistry*, *112*, 457-476.

McGroddy, M. E., Daufresne, T., & Hedin, L. O. (2004). Scaling of C:N:P stoichiometry in forests worldwide: implications of terrestrial redfield-type ratios. *Ecology*, *85*, 2390-2401.

Menge, D. N. L., Levin, S. A., & Hedin, L. O. (2009). Facultative versus obligate nitrogen fixation strategies and their ecosystem consequences. *The American Naturalist*, *174*(4).

Meyerholt, J., & Zaehle, S. (2015). The role of stoichiometric flexibility in modelling forest ecosystem responses to nitrogen fertilization. *New Phytologist*, *208*, 1042-1055. (doi: 10.1111/nph.13547)

Moore, J. C., Berlow, E. L., Coleman, D. C., de Ruiter, P. C., Dong, Q., Hastings, A., ... Wall, D. H. (2004). Detritus, trophic dynamics and biodiversity. *Ecology Letters*, *7*, 584-600.

Moorhead, D. L., & Sinsabaugh, R. L. (2006). A theoretical model of litter decay and microbial interaction. *Ecological Monographs*, *76*, 151-174.

Mooshammer, M., Wanek, W., Zechmeister-Boltenstern, S., & Richter., A. (2014). Stoichiometric imbalances between terrestrial decomposer communities and their resources: mechanisms and implications of microbial adaptations to their resources. *Frontiers in Microbiology*, *5*(22), 1-10.

Mouginot, C., Kawamura, R., Matulich, K. L., Berlemont, R., Allison, S. D., Amend, A. S., & Martiny, A. C. (2014). Elemental stoichiometry of fungi and bacteria strains from grassland leaf litter. *Soil Biology & Biochemistry*, *76*, 278-285.

Moyano, F. E., Kutsch, W. L., & Rebmann, C. (2008). Soil respiration fluxes in relation to photosynthetic activity in broad-leaf and needle-leaf forest stands. *Agricultural and ForestMeteorology*, *148*, 135-143.

Moyano, F. E., Manzoni, S., & Chenu, C. (2013). Responses of soil heterotrophic respiration to moisture availability: An exploration of processes and models. *Soil Biology & Biochemistry*, *59*, 72.85.

Nadelhoffer, K. J., McDowell, W., Boone, R. D., Bowden, R. D., Canary, J. D., Kaye, J., ... Lajtha, K. (2004). The DIRT experiment: litter and root influences on forest soil organic matter stocks and function. In J. D. Foster David R.//Aber (Ed.), *Forests in time: the environmental consequences of 1,000 years of change in New England* (p. 300-315). New Haven, CT: Yale University Press. Retrieved from `http://andrewsforest.oregonstate.edu/pubs/pdf/pub4189.pdf`

Nannipieri, P., Ascher, J., Ceccherini, M. T., Landi, L., Pietramellara, G., & Renella, G. (2017). Microbial diversity and soil functions. *European Journal of Soil Science*, *68*, 12-26.

Nave, L. E., Gough, C. M., Maurer, K. D., Bohrer, G., Hardiman, B. S., Moine, J. L., ... Curtis, P. S. (2011). Disturbance and the resilience of coupled carbon and nitrogen cycling in a north temperate forest. *J. Geophys. Res.*, *116*, G04016. (doi:10.1029/2011JG001758)

Nave, L. E., Vogel, C. S., Gough, C. M., & Curtis, P. S. (2009). Contribution of atmospheric nitrogen deposition to net primary productivity in a northern hardwood forest. *Can. J. For. Res.*, *39*, 1108-1118.

Niu, S., Classen, A. T., Dukes, J. S., Kardol, P., Liu, L., Luo, Y., ... Zaehle, S. (2016). Global patterns and substrate-based mechanisms of the terrestrial nitrogen cycle. *Ecology Letters*, *19*(6), 697-709.

Nottingham, A. T., Turner, B. L., Winter, K., van der Heijden, M. G., & Tanner, E. V. (2010). Arbuscular mycorrhizal mycelial respiration in a moist tropical forest. *New Phytologist*, *186*, 957-967. (doi:10.1111/j.1469-8137.2010.03226.x)

Ojima, D. S., Schimel, D. S., Parton, W. J., & Owensby, C. E. (1994). Long- and short-term effects of fire on nitrogen cycling in tallgrass prairie. *Biogeochemistry*, *24*, 67-84.

Oleson, K. W., Lawrence, D. M., Bonan, G. B., Drewniak, B., Huang, M., Kowen, C. D., ... Thornton, P. E. (2013). *Technical description of version 4.5 of the community land model (CLM)* (Tech. Rep. Nos. NCAR/TN-503+STR). Natl. Cent. for Atmos. Res., Boulder, Colorado.

Orwin, K. H., Kirschbaum, M. U. F., St John, M. G., & Dickie, I. A. (2011). Organic nutrient uptake by mycorrhizal fungi enhances ecosystem carbon storage: a model-based assessment. *Ecology Letters*, *14*, 493-502. (doi: 10.1111/j.1461-0248.2011.01611.x)

Osler, G. H. R., & Sommerkorn, M. (2007). Toward a complete soil c and n cycle: Incorporating the soil fauna. *Ecology*, *88*, 1611-1621.

Pappas, C., Fatichi, S., & Burlando, P. (2016). Modeling terrestrial carbon and water dynamics across climatic gradients: does plant diversity matter? *New Phytologist*, *209*, 137-151. (doi: 10.1111/nph.13590)

Pappas, C., Fatichi, S., Leuzinger, S., Wolf, A., & Burlando, P. (2013, April). Sensitivity analysis of a process-based ecosystem model: Pinpointing parameterization and structural issues. *Journal of Geophysical Research: Biogeosciences*, *118*(2), 505–528. doi: 10.1002/jgrg.20035

Parton, W. J., Scurlock, J. M. O., Ojima, D. S., Gilmanov, T. G., Scholes, R. J., Schimel, D. S., ... Kinyamario, J. I. (1993). Observations and modelling of biomass and soil organic matter dynamics for the grassland biome worldwide. *Global Biogeochemical Cycles*, *7*, 785-809.

Parton, W. J., Stewart, J. W. B., & Cole, C. V. (1988). Dynamics of C, N, P and S in grassland soils - a model. *Biogeochemistry*, *5*, 109-131.

Paschalis, A., Fatichi, S., Katul, G. G., & Ivanov, V. Y. (2015). Cross-scale impact of climate temporal variability on ecosystem water and carbon fluxes. *Journal of Geophysical Research-Biogeosciences*, *120*, 1716-1740. (doi: 10.1002/2015JG003002)

Paschalis, A., Fatichi, S., Pappas, C., & Or, D. (2018). Covariation of vegetation and climate constrains present and future T/ET variability. *Environmental Research Letters*, *13*, 104012. (doi:10.1088/1748-9326/aae267)

Phillips, R. P., Brzostek, E. R., & Midgley, M. G. (2013). The mycorrhizal-associated nutrient economy: a new framework for predicting carbon-nutrient couplings in temperate forests. *New Phytologist*, *199*, 41-51.

Poorter, H. (1994). A whole plant perspective on carbon-nitrogen interactions. In J. Roy & E. Garnier (Eds.), (p. 111-127). SPB Academic Publishing bv, The Hague, The Netherlands.

1547 Poorter, H., & Villar, R. (1997). Plant resource allocation. In F. A. Bazzaz &
1548 B. Jones (Eds.), (p. 39-72). Academic Press, New York.
1549 Porporato, A., D'Odorico, P., Laio, F., & Rodriguez-Iturbe, I. (2003). Hydrologic
1550 controls on soil carbon and nitrogen cycles. I. Modeling scheme. *Advances in*
1551 *Water Resources*, *26*, 45-58.
1552 Raich, J. W., & Nadelhoffer, K. J. (1989). Belowground carbon allocation in forest
1553 ecosystems: global trends. *Ecology*, *70*, 1346-1354.
1554 Raich, J. W., & Schlesinger, W. (1992). The global carbon dioxide flux in soil respi-
1555 ration and its relationship to vegetation and climate. *Tellus B*, *44*(2), 81-99.
1556 Read, D. J., Leake, J. R., & Perez-Moreno, J. (2004). Mycorrhizal fungi as drivers
1557 of ecosystem processes in heathland and boreal forest biomes. *Canadian Jour-*
1558 *nal of Botany*, *82*, 1243-1263.
1559 Reed, S. C., Townsend, A. R., Davidson, E. A., & Cleveland, C. C. (2012). Stoichio-
1560 metric patterns in foliar nutrient resorption across multiple scales. *New Phytol-*
1561 *ogist*, *196*, 173-180. (doi: 10.1111/j.1469-8137.2012.04249.x)
1562 Reich, P. B., Grigal, D. F., Aber, J. D., & Gower, S. T. (1997). Nitrogen mineraliza-
1563 tion and productivity in 50 hardwood and conifer stands on diverse soils. *Ecol-*
1564 *ogy*, *78*, 335-347.
1565 Reich, P. B., & Oleksyn, J. (2004). Global patterns of plant leaf N and P in relation
1566 to temperature and latitude. *P. Natl. Acad. Sci. USA*, *101*, 11001-11006.
1567 Robertson, A. D., Paustian, K., Ogle, S., Wallenstein, M. D., Lugato, E., & Cotrufo,
1568 M. F. (2019). Unifying soil organic matter formation and persistence frame-
1569 works: the mems model. *Biogeosciences*, *In press*, In press.
1570 Roumet, C., Birouste, M., Picon-Cochard, C., Ghestem, M., Osman, N., Vrignon-
1571 Brenas, S., ... Stokes, A. (2016). Root structure-function relationships in
1572 74 species: evidence of a root economics spectrum related to carbon economy.
1573 *New Phytologist*, *210*(3), 815-826.
1574 Rousk, J., & Frey, S. D. (2015). Revisiting the hypothesis that fungal-to-bacterial
1575 dominance characterizes turnover of soil organic matter and nutrients. *Ecologi-*
1576 *cal Monographs*, *85*(3), 457-472.
1577 Ruimy, A., Dedieu, G., & Saugier, B. (1996). TURC: A diagnostic model of conti-
1578 nental gross primary productivity and net primary productivity. *Global Biogeo-*
1579 *chemical Cycles*, *10*, 269-285.
1580 Ruiz, S., Or, D., & Schymanski, S. J. (2015). Soil penetration by earthworms and
1581 plant roots-mechanical energetics of bioturbation of compacted soils. *PLoS*
1582 *ONE*, *10*(6), e0128914. (doi:10.1371/journal.pone.0128914)
1583 Runyan, C. W., & D'Odorico, P. (2012). Hydrologic controls on phosphorus dynam-
1584 ics: A modeling framework. *Advances in Water Resources*, *35*, 94-109.
1585 Ryan, M. G. (1991). Effects of cllimate change on plant respiration. *Ecological Ap-*
1586 *plications*, *1*(2), 157-167.
1587 Sardans, J., & Penuelas, J. (2015). Potassium: a neglected nutrient in global change.
1588 *Global Ecology and Biogeography*, *24*, 261-275.
1589 Sato, H., Itoh, A., & Kohyama, T. (2007). SEIB-DGVM: A new Dynamic Global
1590 Vegetation Model using a spatially explicit individual-based approach. *Ecologi-*
1591 *cal Modelling*, *200*, 279-307.
1592 Schimel, J. P. (2013). Microbes and global carbon. *Nature Climate Change*, *3*, 867-
1593 868.
1594 Schimel, J. P., Becerra, C. A., & Blankinship, J. (2017). Estimating decay dynamics
1595 for enzyme activities in soils from different ecosystems. *Soil Biology and Bio-*
1596 *chemistry*, *114*, 5-11.
1597 Schimel, J. P., & Weintraub, M. N. (2003). The implications of exoenzyme activity
1598 on microbial carbon and nitrogen limitation in soil: a theoretical model. *Soil*
1599 *Biology and Biochemistry*, *35*, 549-563.
1600 Schmid, H. P., Su, H. B., Vogel, C. S., & Curtis, P. S. (2003). Ecosystem-
1601 atmosphere exchange of carbon dioxide over a mixed hardwood forest in

northern lower michigan. *Journal of Geophysical Research - Atmospheres*, *108*(D14), 4417.

Schmidt, M. W. I., Torn, M. S., Abiven, S., Dittmar, T., Guggenberger, G., Janssens, I. A., ... Trumbore, S. E. (2011). Persistence of soil organic matter as an ecosystem property. *Nature*, *478*, 49-56.

Selim, H. M., Mansell, R. S., & Zelazny, L. (1976). Modeling reactions and transport of potassium in soils. *Soil Sci.*, *122*, 77-84.

Serna-Chavez, H. M., Fierer, N., & van Bodegom, P. M. (2013). Global drivers and patterns of microbial abundance in soil. *Global Ecology and Biogeography*, *22*, 1162-1172.

Sherrod, L. A., Peterson, G. A., Westfall, D. G., & Ahuja, L. R. (2005). Soil organic carbon pools after 12 years in no-till dryland agroecosystems. *Soil Sci. Soc. Am. J.*, *69*, 1600-1608.

Shi, M., Fisher, J. B., Brzostek, E. R., & Phillips, R. P. (2016). Carbon cost of plant nitrogen acquisition: global carbon cycle impact from an improved plant nitrogen cycle in the Community Land Model. *Global Change Biology*, *22*, 1299-1314. (doi: 10.1111/gcb.13131)

Sinsabaugh, R. L., Belnap, J., Findlay, S. G., Shah, J. J. F., Hill, B. H., Kuehn, K. A., ... Warnock, D. D. (2014). Extracellular enzyme kinetics scale with resource availability. *Biogeochemistry*, *121*, 287-304. (doi:10.1007/s10533-014-0030-y)

Sinsabaugh, R. L., Manzoni, S., Moorhead, D. L., & Richter, A. (2013). Carbon use efficiency of microbial communities: stoichiometry, methodology and modelling. *Ecology Letters*, *16*, 930-939. (doi: 10.1111/ele.12113)

Sinsabaugh, R. L., Shah, J. J. F., Findlay, S. G., Kuehn, K. A., & Moorhead, D. L. (2015). Scaling microbial biomass, metabolism and resource supply. *Biogeochemistry*, *122*, 175-190. (doi:10.1007/s10533-014-0058-z)

Sistla, S. A., & Schimel, J. P. (2012). Stoichiometric flexibility as a regulator of carbon and nutrient cycling in terrestrial ecosystems under change. *New Phytologist*, *196*, 68-78. (doi: 10.1111/j.1469-8137.2012.04234.x)

Sitch, S., Smith, B., Prentice, I. C., Arneth, A., Bondeau, A., Cramer, W., ... Venevski, S. (2003). Evaluation of ecosystem dynamics, plant geography and terrestrial carbon cycling in the LPJ dynamic global vegetation model. *Global Change Biology*, *9*, 161-185.

Six, J., Conant, R. T., Paul, E. A., & Paustian, K. (2002). Stabilization mechanisms of soil organic matter: Implications for c-saturation of soils. *Plant and Soil*, *241*, 155-176.

Six, J., Frey, S. D., Thiet, R. K., & Batten, K. M. (2006). Bacterial and fungal contributions to carbon sequestration in agroecosystems. *Soil Sci. Soc. Am. J.*, *70*, 555-569.

Six, J., Guggenberger, G., Paustian, K., Haumaier, L., Elliott, E. T., & Zech, W. (2001). Sources and composition of soil organic matter fractions between and within soil aggregates. *European Journal of Soil Science*, *52*, 607-618.

Smith, P., Smith, J. U., Powlson, D. S., McGill, W. B., Arah, J. R. M., Chertov, O. G., ... Whitmore, A. P. (1997). A comparison of the performance of nine soil organic matter models using datasets from seven long-term experiments. *Geoderma*, *81*, 153-225.

Smith, S. E., & Read, D. J. (2008). *Mycorrhizal symbiosis*. Academic Press, London, UK.

Smith, S. E., & Smith, F. A. (2011). Roles of arbuscular mycorrhizas in plant nutrition and growth: New paradigms from cellular to ecosystem scales. *Annu. Rev. Plant Biol.*, *62*, 227-250.

Sparks, D. L. (1987). Potassium dynamics in soils. *Adv Soil Sci*, *6*, 1-63.

Sparks, D. L., & Carski, T. H. (1985). Kinetics of potassium exchange in heterogeneous systems. *Appl. Clay Sci*, *1*, 89-101.

Sparks, D. L., & Huang, P. M. (1985). Potassium in agriculture. In R. D. Munson (Ed.), (p. 201-276). American Society of Agronomy, Crop Science Society of America, and Soil Science Society of America, Madison, WI.

Stewart, C. E., Paustian, K., Conant, R. T., Plante, A. F., & Six, J. (2007). Soil carbon saturation: concept, evidence and evaluation. *Biogeochemistry*, *86*, 19-31. (doi:10.1007/s10533-007-9140-0)

Stewart, C. E., Plante, A. F., Paustian, K., Conant, R. T., & Six, J. (2007). Soil carbon saturation: Linking concept and measurable carbon pools. *Soil Sci. Soc. Am. J.*, *72*, 379-392. (doi:10.2136/sssaj2007.0104)

Talbot, J. M., Bruns, T. D., Smith, D. P., Branco, S., Glassman, S. I., Erlandson, S., ... Peay, K. G. (2013). Independent roles of ectomycorrhizal and saprophytic communities in soil organic matter decomposition. *Soil Biology & Biochemistry*, *57*, 282-291.

Talbot, J. M., & Treseder, K. K. (2012). Interactions among lignin, cellulose, and nitrogen drive litter chemistry-decay relationships. *Ecology*, *93*(2), 345-354.

Tang, J. Y., & Riley, W. J. (2015). Weaker soil carbon-climate feedbacks resulting from microbial and abiotic interactions. *Nature Climate Change*, *5*, 56-60.

Tang, J. Y., Riley, W. J., Koven, C. D., & Subin, Z. M. (2013). CLM4-BeTR, a generic biogeochemical transport and reaction module for CLM4: model development, evaluation, and application. *Geosci. Model Dev.*, *6*, 127-140.

Tecon, R., & Or, D. (2017). Biophysical processes supporting the diversity of microbial life in soil. *FEMS Microbiology Reviews*, *41*, 599-623.

Thomas, H., & Stoddart, J. L. (1980). Leaf senescence. *Annual Review of Plant Physiology*, *31*, 83-111. (doi:10.1146/annurev.pp.31.060180.000503)

Thomas, S. C., & Martin, A. R. (2012). Carbon content of tree tissues: A synthesis. *Forests*, *3*, 332-352. (doi:10.3390/f3020332)

Thornton, P. E., Lamarque, J.-F., Rosenbloom, N. A., & Mahowald, N. M. (2007). Influence of carbon-nitrogen cycle coupling on land model response to CO_2 fertilization and climate variability. *Global Biogeochemical Cycles*, *21*(GB4018). (doi:10.1029/2006GB002868)

Todd-Brown, K. E. O., Randerson, J. T., Hopkins, F., Arora, V., Hajima, T., Jones, C., ... Allison, S. D. (2014). Changes in soil organic carbon storage predicted by Earth system models during the 21st century. *Biogeosciences*, *11*, 2341-2356.

Todd-Brown, K. E. O., Randerson, J. T., Post, W. M., Hoffman, F. M., Tarnocai, C., Schuur, E. A. G., & Allison, S. D. (2013). Causes of variation in soil carbon simulations from CMIP5 Earth system models and comparison with observations. *Biogeosciences*, *10*, 1717-1736.

Tomè, E., Ventura, M., Folegot, S., Zanotelli, D., Montagnani, L., Mimmo, T., ... Scandellari, F. (2016). Mycorrhizal contribution to soil respiration in an apple orchard. *Applied Soil Ecology*, *101*, 165-173.

Tonitto, C., Goodale, C. L., Weiss, M. S., Frey, S. D., & Ollinger, S. V. (2014). The effect of nitrogen addition on soil organic matter dynamics: a model analysis of the harvard forest chronic nitrogen amendment study and soil carbon response to anthropogenic n deposition. *Biogeochemistry*, *117*(2-3), 431-454.

Treseder, K. K. (2008). Nitrogen additions and microbial biomass: a meta-analysis of ecosystem studies. *Ecology Letters*, *11*, 1111-1120.

Trumbore, S. E., & Czimczik, C. I. (2008). An uncertain future for soil carbon. *Science*, *321*, 1455-1456.

Urbanski, S., Barford, C., Wofsy, S., Kucharik, C., Pyle, E., Budney, J., ... Munger, J. W. (2007). Factors controlling CO_2 exchange on timescales from hourly to decadal at Harvard Forest. *Journal of Geophysical Research*, *112*(G02020). (doi:10.1029/2006JG000293)

Vergutz, L., Manzoni, S., Porporato, A., Novais, R. F., & Jackson, R. B. (2012). Global resorption efficiencies and concentrations of carbon and nutrients in

leaves of terrestrial plants. *Ecological Monographs*, *82*, 205-220.

Vet, R., Artz, R. S., Carou, S., Shawa, M., Ro, C.-U., Aas, W., ... Reid, N. W. (2014). A global assessment of precipitation chemistry and deposition of sulfur, nitrogen, sea salt, base cations, organic acids, acidity and ph, and phosphorus. *Atmospheric Environment*, *93*, 3-100.

Vitousek, P. M., Porder, S., Houlton, B. Z., & Chadwick, O. A. (2010). Terrestrial phosphorus limitation: mechanisms, implications, and nitrogen-phosphorus interactions. *Ecological Applications*, *20*(1), 5-15.

Wadman, W. P., & de Haan, S. (1997). Decomposition of organic matter from 36 soils in a long-term pot experiment. *Plant and Soil*, *189*, 289-301.

Wallenstein, M. D., McNulty, S., Fernandez, I. J., Boggs, J., & Schlesinger, W. H. (2006). Nitrogen fertilization decreases forest soil fungal and bacterial biomass in three long-term experiments. *Forest Ecology and Management*, *222*, 459-468.

Wan, S., Hui, D., & Luo, Y. (2001). Fire effects on nitrogen pools and dynamics in terrestrial ecosystems: a meta-analysis. *Ecological Applications*, *11*, 1349-1365.

Wang, G., & Post, W. M. (2012). A theoretical reassessment of microbial maintenance and implications for microbial ecology modeling. *FEMS Microbiology Ecology*, *81*, 610-617.

Wang, G., Post, W. M., & Mayes, M. A. (2013). Development of microbial-enzyme-mediated decomposition model parameters through steady-state and dynamic analyses. *Ecological Applications*, *23*(1), 255-272.

Wang, G., Post, W. M., Mayes, M. A., Frerichs, J. T., & Jagadamma, S. (2012). Parameter estimation for models of ligninolytic and cellulolytic enzyme kinetics. *Soil Biology and Biochemistry*, *48*, 28-38.

Wang, G.-H., Jin, J., Liu, J.-J., Chen, X.-L., Liu, J.-D., & Liu, X.-B. (2009). Bacterial community structure in a mollisol under long-term natural restoration, cropping, and bare fallow history estimated by PCR-DGGE. *Pedosphere*, *19*, 156-165.

Wang, Y.-P., Houlton, B. Z., & Field, C. B. (2007). A model of biogeochemical cycles of carbon, nitrogen, and phosphorus including symbiotic nitrogen fixation and phosphatase production. *Global Biogeochemical Cycles*, *21*(GB1018). (doi:10.1029/2006GB002797)

Wardle, D. A. (1992). A comparative assessment of factors which influence microbial biomass carbon and nitrogen levels in soil. *Biol. Rev.*, *67*, 321-358.

Waring, B. G., Averill, C., & Hawkes, C. V. (2013). Differences in fungal and bacterial physiology alter soil carbon and nitrogen cycling: insights from meta-analysis and theoretical models. *Ecology Letters*, *16*, 887-894.

Whalen, J. K., Paustian, K. H., & Parmelee, R. W. (1999). Simulation of growth and flux of carbon and nitrogen through earthworms. *Pedobiologia*, *43*, 537-546.

Wieder, W. R., Allison, S. D., Davidson, E. A., Georgiou, K., Hararuk, O., He, Y., ... Xu, X. (2015). Explicitly representing soil microbial processes in Earth system models. *Global Biogeochem. Cycles*, *29*, 1782-1800.

Wieder, W. R., Bonan, G. B., & Allison, S. D. (2013). Global soil carbon projections are improved by modelling microbial processes. *Nature Climate Change*, *3*, 909-912.

Wieder, W. R., Grandy, A. S., Kallenbach, C. M., & Bonan, G. B. (2014). Integrating microbial physiology and physio-chemical principles in soils with the MIcrobial-MIneral Carbon Stabilization (MIMICS) model. *Biogeosciences*, *11*, 3899-3917. (doi:10.5194/bg-11-3899-2014)

Wieder, W. R., Grandy, A. S., Kallenbach, C. M., Taylor, P. G., & Bonan, G. B. (2015). Representing life in the earth system with soil microbial functional traits in the MIMICS model. *Geosci. Model Dev.*, *8*, 1789-1808.

(doi:10.5194/gmd-8-1789-2015)

Witter, E., & Kanal, A. (1998). Characteristics of the soil microbial biomass in soils from a long-term field experiment with different levels of c input. *Applied Soil Ecology*, *10*, 37-49.

Xu, X., Schimel, J. P., Janssens, I. A., Song, X., Song, C., Yu, G., ... Thornton, P. E. (2017). Global pattern and controls of soil microbial metabolic quotient. *Ecological Monographs*, *87*, 429-441.

Xu, X., Schimel, J. P., Thornton, P. E., Song, X., Yuan, F., & Goswami, S. (2014). Substrate and environmental controls on microbial assimilation of soil organic carbon: a framework for earth system models. *Ecology Letters*, *17*, 547-555.

Xu, X., Thornton, P. E., & Post, W. M. (2013). A global analysis of soil microbial biomass carbon, nitrogen and phosphorus in terrestrial ecosystems. *Global Ecology and Biogeography*, *22*, 737-749.

Xu-Ri, & Prentice, I. C. (2008). Terrestrial nitrogen cycle simulation with a dynamic global vegetation model. *Global Change Biol.*, *14*, 1745-1764. (doi:10.1111/j.1365- 2486.2008.01625.x)

Yang, X., Post, W. M., Thornton, P. E., & Jain, A. (2013). The distribution of soil phosphorus for global biogeochemical modeling. *Biogeosciences*, *10*, 2525-2537. (doi:10.5194/bg-10-2525-2013)

Yang, X., Thornton, P. E., Ricciuto, D. M., & Post, W. M. (2014). The role of phosphorus dynamics in tropical forests - a modeling study using CLM-CNP. *Biogeosciences*, *11*, 1667-1681. (doi:10.5194/bg-11-1667-2014)

Yang, X., Wittig, V., Jain, A. K., & Post, W. (2009). Integration of nitrogen cycle dynamics into the integrated science assessment model for the study of terrestrialecosystem responses to global change. *Global Biogeochemical Cycles*, *23*(GB4029). (doi:10.1029/2009GB003474)

Yu, W.-T., Bi, M.-L., Xu, Y.-G., Zhou, H., Ma, Q., & Jiang, C.-M. (2013). Microbial biomass and community composition in a luvisol soil as influenced by long-term land use and fertilization. *Catena*, *107*, 89-95.

Zaehle, S., & Dalmonech, D. (2011). Carbon-nitrogen interactions on land at global scales: current understanding in modelling climate biosphere feedbacks. *Current Opinion in Environmental Sustainability*, *3*, 311-320. (doi:10.1016/j.cosust.2011.08.008)

Zaehle, S., & Friend, A. (2010). Carbon and nitrogen cycle dynamics in the O-CN land surface model: 1. model description, site-scale evaluation, and sensitivity to parameter estimates. *Global Biogeochemical Cycles*, *24*(GB1005). (doi:10.1029/2009GB003521)

Zaehle, S., Medlyn, B. E., De Kauwe, M. G., Walker, A. P., Dietze, M. C., Hickler, T., ... Norby, R. J. (2014). Evaluation of 11 terrestrial carbon-nitrogen cycle models against observations from two temperate Free-Air CO_2 enrichment studies. *New Phytologist*, *202*, 803-822. (doi:10.1111/nph.12697)

Zak, D. R., Tilman, D., Parmenter, R. R., Rice, C. W., Fisher, F. M., Vose, J., ... Martin, C. W. (1994). Plant production and soil microorganisms in late-successional ecosystems: A continental-scale study. *Ecology*, *75*(8), 2333-2347.

Zhang, H.-Y., Lu, X.-T., Hartmann, H., Keller, A., Han, X.-G., Trumbore, S., & Phillips, R. P. (2018). Foliar nutrient resorption differs between arbuscular mycorrhizal and ectomycorrhizal trees at local and global scales. *Global Ecol Biogeogr.*, *27*(7), 875-885.

Zhu, Q., Riley, W. J., Tang, J., & Koven, C. D. (2016). Multiple soil nutrient competition between plants, microbes, and mineral surfaces: model development, parameterization, and example applications in several tropical forests. *Biogeosciences*, *13*, 341-363.

Figure 1.

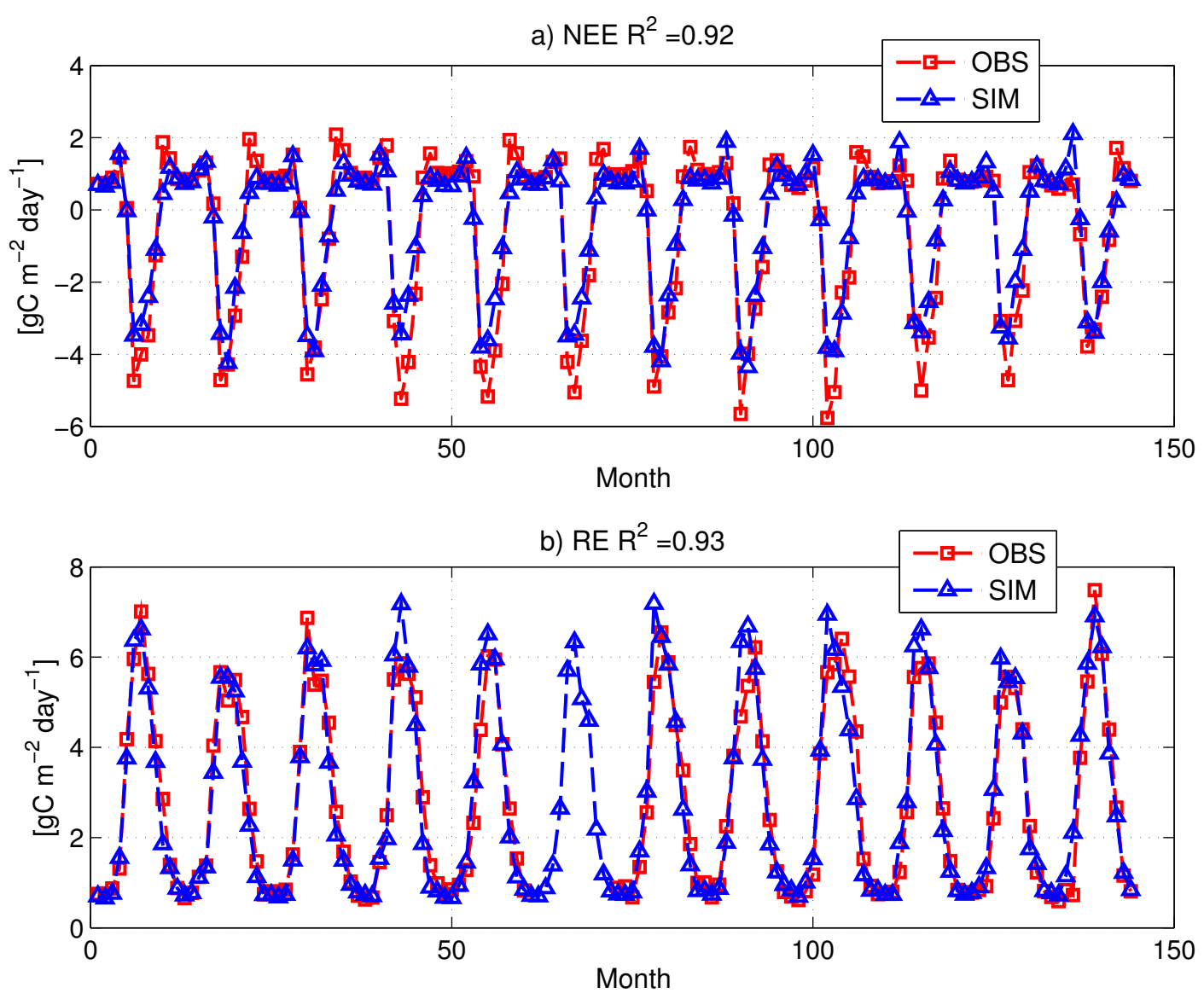
a) NEE R2 =0.92
OBS
SIM
[gC m−2 day−1]
Month
b) RE R2 =0.93
OBS
SIM
[gC m−2 day−1]
Month

Figure 2.

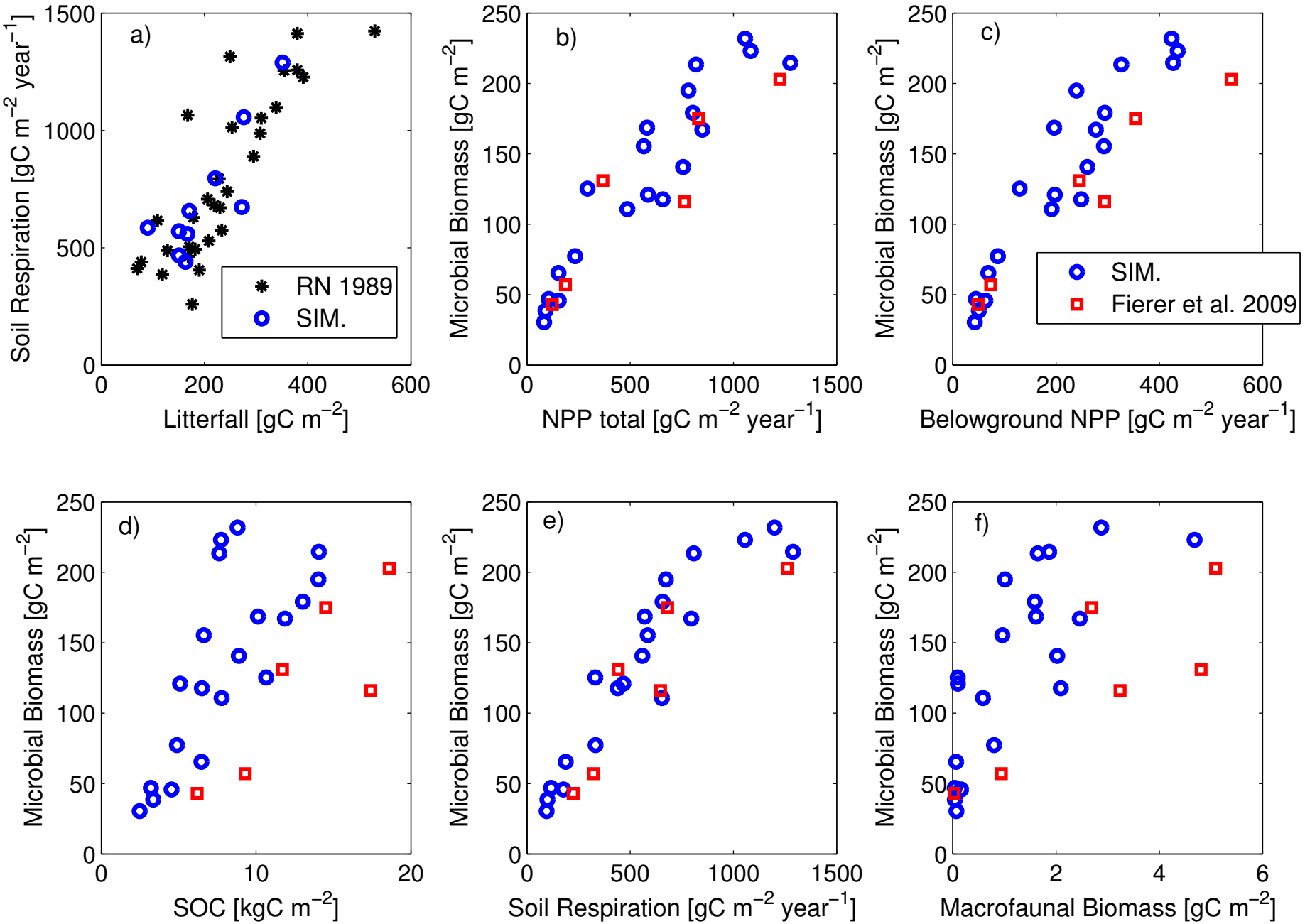
a)
b)
c)
d)
e)
f)
Soil Respiration [gC m^{-2} year^{-1}]
Litterfall [gC m^{-2}]
RN 1989
SIM.
Microbial Biomass [gC m^{-2}]
NPP total [gC m^{-2} year^{-1}]
Belowground NPP [gC m^{-2} year^{-1}]
SIM.
Fierer et al. 2009
SOC [kgC m^{-2}]
Macrofaunal Biomass [gC m^{-2}]

Figure 3.

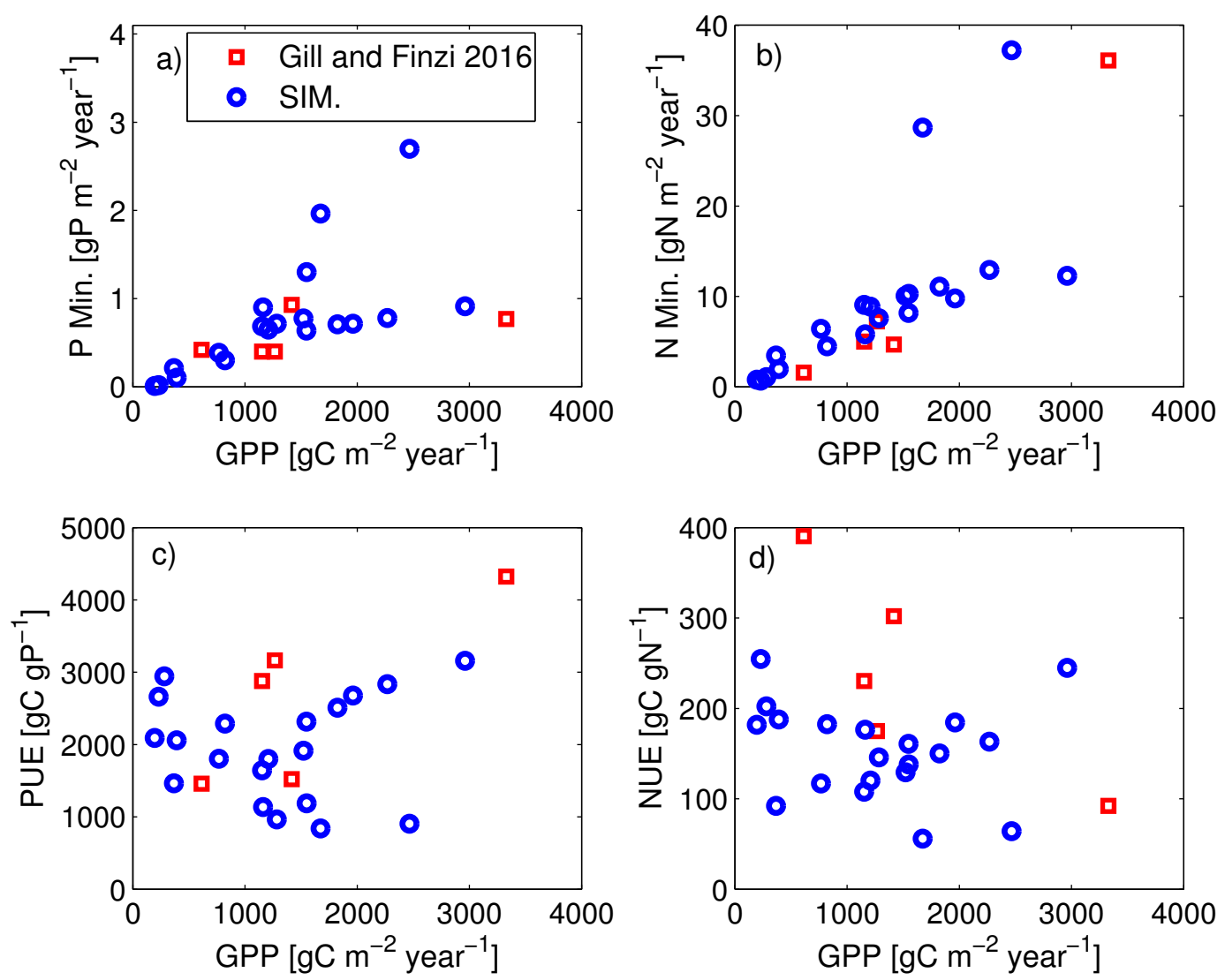
a)
Gill and Finzi 2016
SIM.
P Min. [gP m^{-2} year^{-1}]
GPP [gC m^{-2} year^{-1}]
b)
N Min. [gN m^{-2} year^{-1}]
GPP [gC m^{-2} year^{-1}]
c)
PUE [gC gP^{-1}]
GPP [gC m^{-2} year^{-1}]
d)
NUE [gC gN^{-1}]
GPP [gC m^{-2} year^{-1}]

Figure 4.

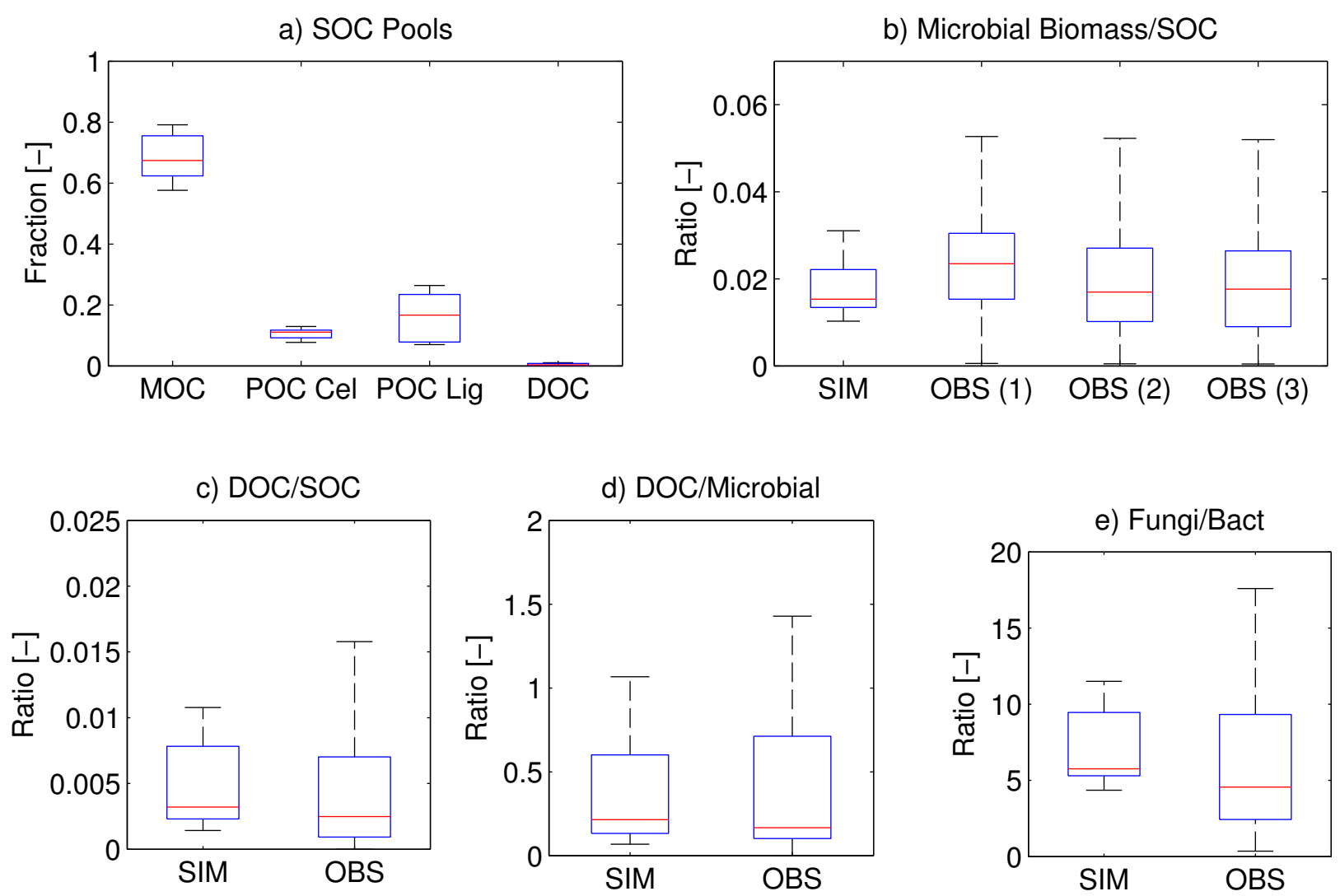
a) SOC Pools
Fraction [–]
1
0.8
0.6
0.4
0.2
0
MOC
POC Cel
POC Lig
DOC
b) Microbial Biomass/SOC
Ratio [–]
0.06
0.04
0.02
0
SIM
OBS (1)
OBS (2)
OBS (3)
c) DOC/SOC
Ratio [–]
0.025
0.02
0.015
0.01
0.005
0
SIM
OBS
d) DOC/Microbial
Ratio [–]
2
1.5
1
0.5
0
SIM
OBS
e) Fungi/Bact
Ratio [–]
20
15
10
5
0
SIM
OBS

Figure 5.

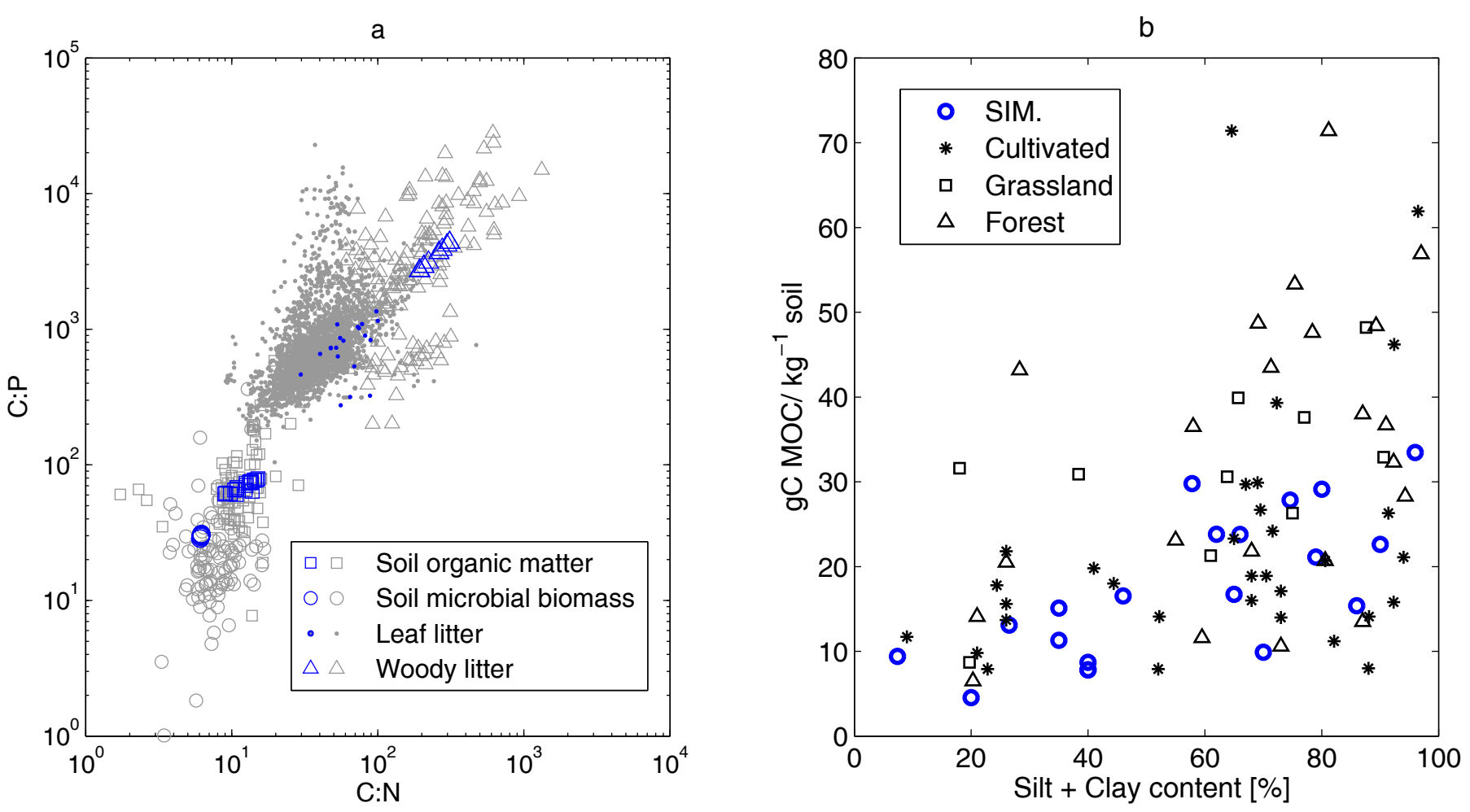
a
C:P
C:N
Soil organic matter
Soil microbial biomass
Leaf litter
Woody litter
b
gC MOC/ kg^{-1} soil
Silt + Clay content [%]
SIM.
Cultivated
Grassland
Forest

Figure 6.

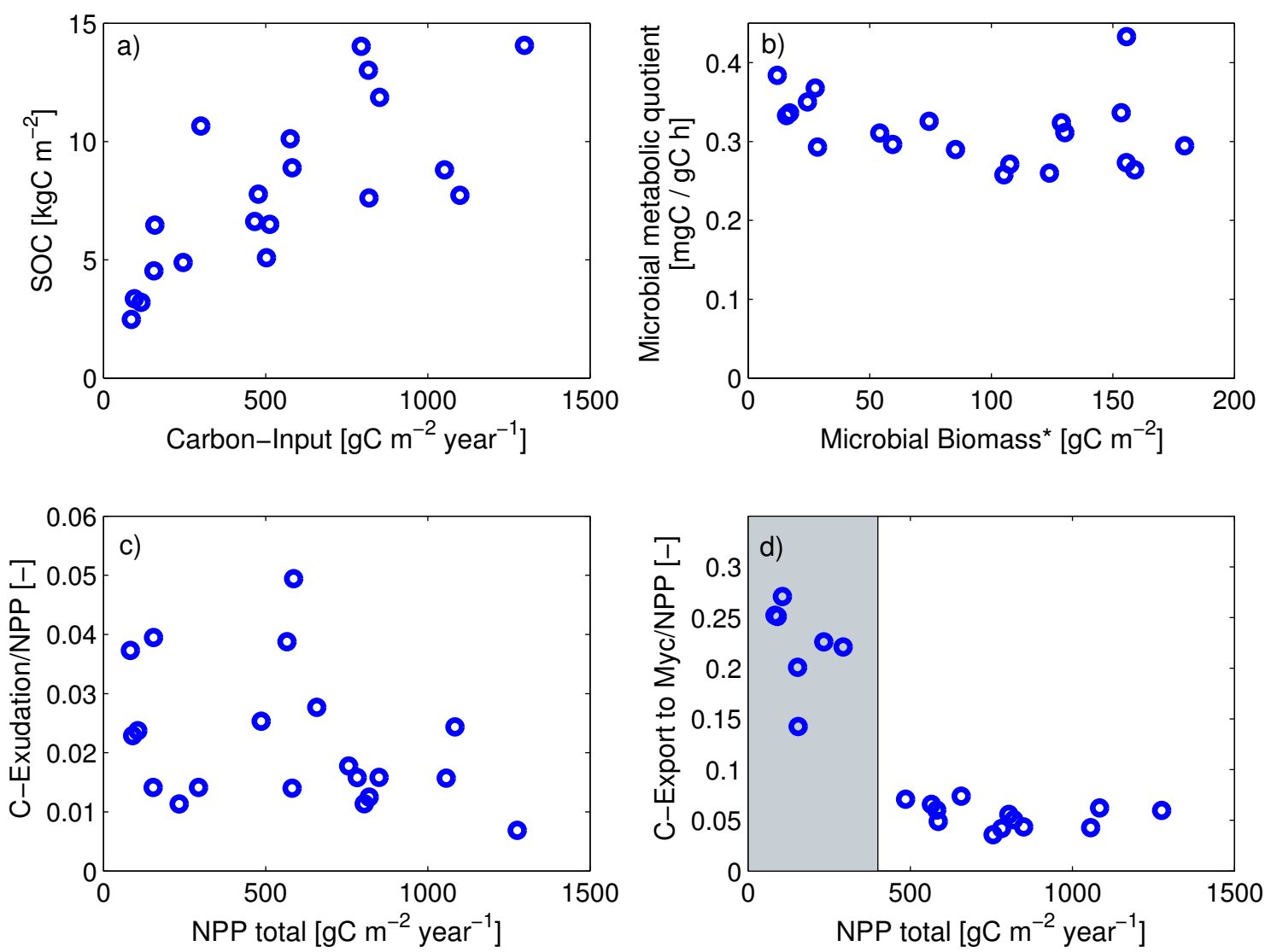
a)
SOC [kgC m^{-2}]
Carbon−Input [gC m^{-2} year^{-1}]
b)
Microbial metabolic quotient [mgC / gC h]
Microbial Biomass* [gC m^{-2}]
c)
C−Exudation/NPP [−]
NPP total [gC m^{-2} year^{-1}]
d)
C−Export to Myc/NPP [−]
NPP total [gC m^{-2} year^{-1}]

Figure 7.

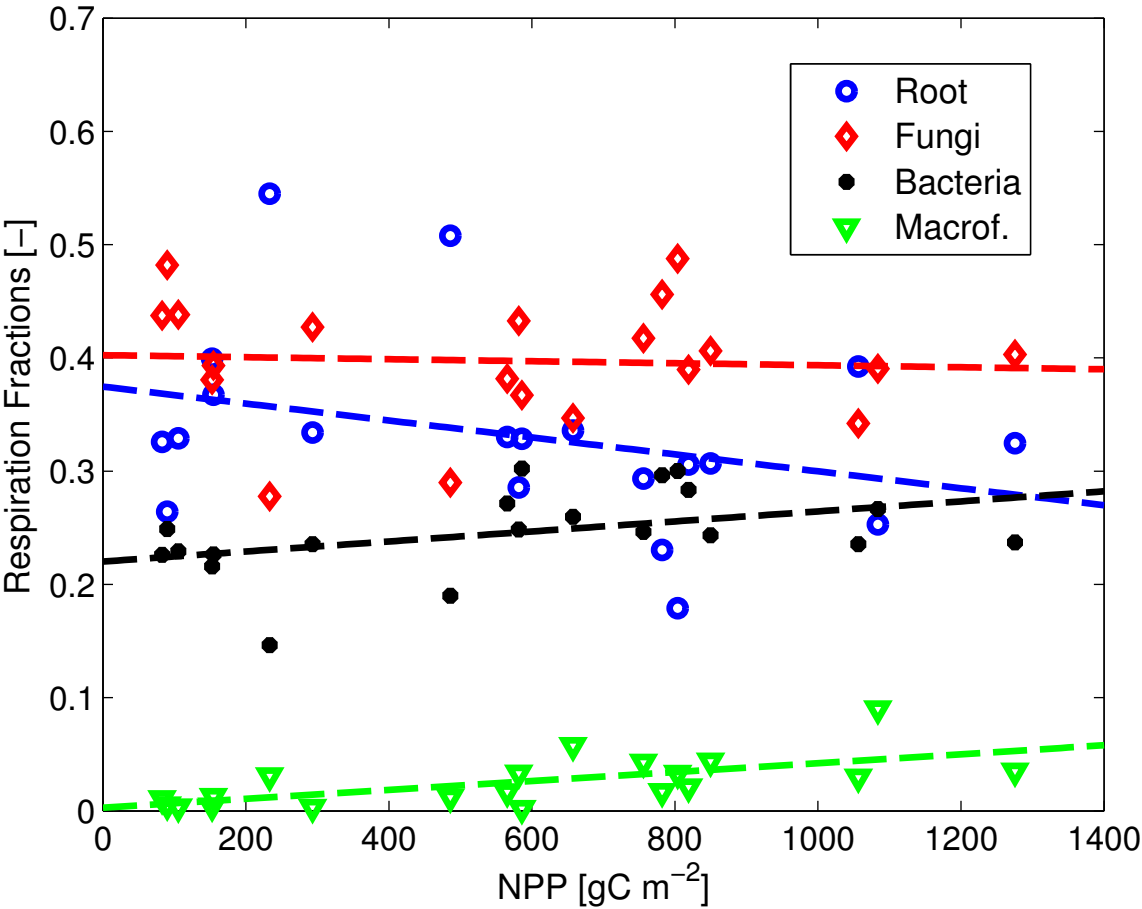
Root
Fungi
Bacteria
Macrof.
Respiration Fractions [–]
NPP [gC m^{-2}]
0.7
0.6
0.5
0.4
0.3
0.2
0.1
0
0
200
400
600
800
1000
1200
1400

Figure 8.

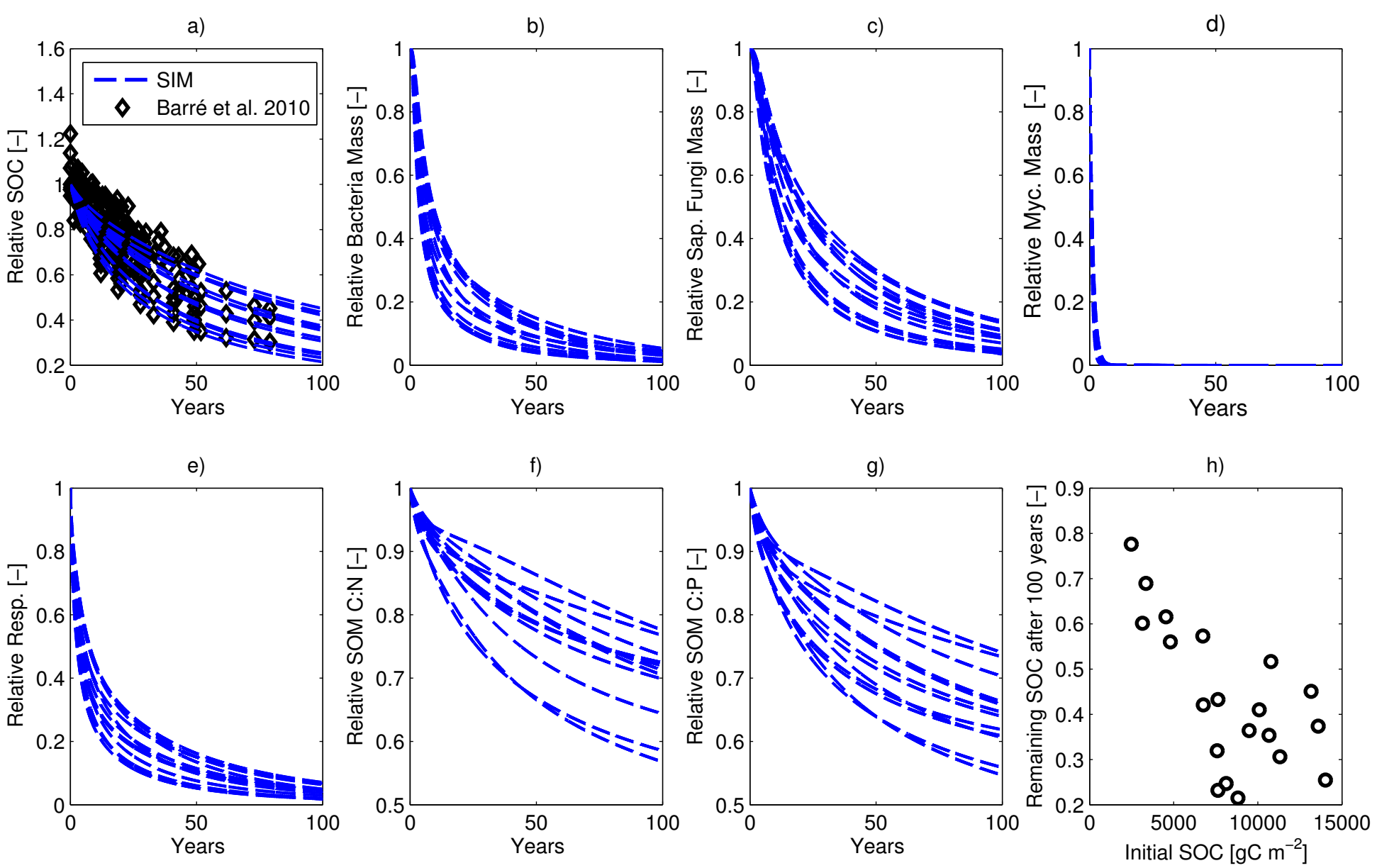
a)
b)
c)
d)
e)
f)
g)
h)
SIM
Barré et al. 2010
Relative SOC [–]
Relative Bacteria Mass [–]
Relative Sap. Fungi Mass [–]
Relative Myc. Mass [–]
Relative Resp. [–]
Relative SOM C:N [–]
Relative SOM C:P [–]
Remaining SOC after 100 years [–]
Years
Initial SOC [gC m^{-2}]

Figure 9.

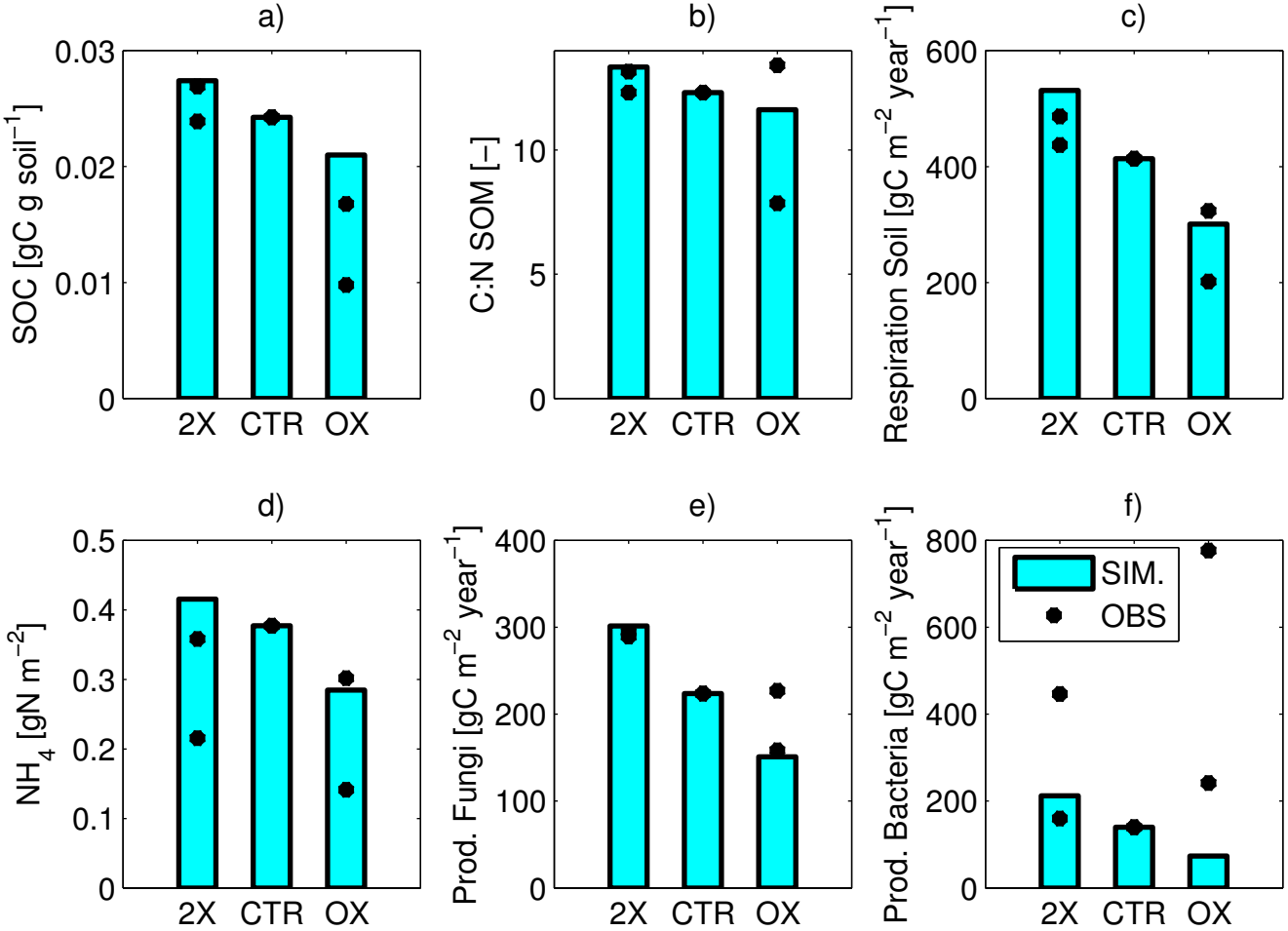
a)
b)
c)
d)
e)
f)
SOC [gC g soil^{-1}]
C:N SOM [–]
Respiration Soil [gC m^{-2} year^{-1}]
NH$_4$ [gN m^{-2}]
Prod. Fungi [gC m^{-2} year^{-1}]
Prod. Bacteria [gC m^{-2} year^{-1}]
0.03
0.02
0.01
0
10
5
600
400
200
0.5
0.4
0.3
0.2
0.1
300
100
800
2X
CTR
OX
SIM.
OBS

Figure 10.

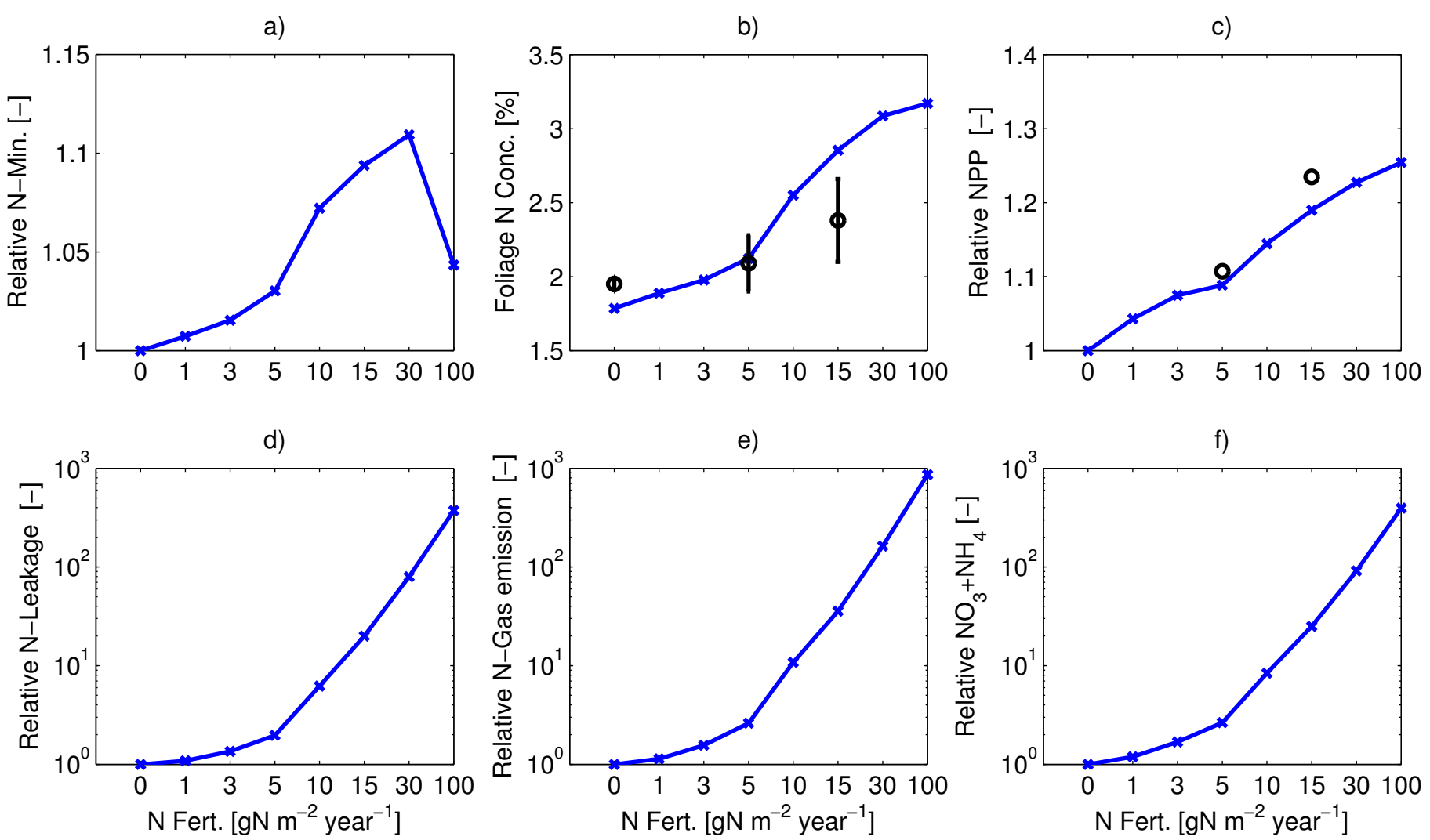
a)
b)
c)
d)
e)
f)
Relative N–Min. [–]
Foliage N Conc. [%]
Relative NPP [–]
Relative N–Leakage [–]
Relative N–Gas emission [–]
Relative NO3+NH4 [–]
N Fert. [gN m−2 year−1]
0 1 3 5 10 15 30 100